# Microwave Materials for Defense and Aerospace Applications

**5**

J. Varghese, N. Joseph, H. Jantunen, S. K. Behera, H. T. Kim, and M. T. Sebastian

## Contents

J. Varghese (✉) · N. Joseph · H. Jantunen
Microelectronics Research Unit, University of Oulu, Oulu, Finland
e-mail: jobin.var@gmail.com; ninajoseph11@gmail.com; heli.jantunen@oulu.fi

S. K. Behera
Department of Electronics and Communication Engineering, NIT Rourkela, Rourkela, India
e-mail: skbehera@nitrkl.ac.in

H. T. Kim · M. T. Sebastian
Korean Institute for Ceramic Engineering and Technology, Jinju-si, South Korea
e-mail: hytek@kicet.re.kr; mailadils@yahoo.com

**Abstract**

Microwave materials are fundamental building blocks for defense and aerospace applications, which have been used as dielectric resonators, radomes, multilayer packages, electromagnetic shield, and so on. These materials and devices made of them should survive in harsh environmental conditions, and hence the availability of suitable materials is limited. Microwave materials are used for signal propagation as well as shielding unwanted signals in military and aerospace applications depending on their properties. The essential material characteristics required for signal propagation applications are very low relative permittivity, low dielectric loss, low-temperature variation of relative permittivity/resonant frequency, and low coefficient of thermal expansion. The materials used for these applications are in the form of substrates, foams, inks, bulk resonators, high-temperature co-fired ceramics (HTCC), low-temperature co-fired ceramics (LTCC), printed circuit boards (PCBs), etc. The materials should absorb or reflect microwaves for electromagnetic interference (EMI) shielding applications. The present chapter gives an overview of microwave material requirements, properties, and their applications in antennas, filters, and oscillators in the military and aerospace sector.

**Keywords**

Microwave materials · HTCC · LTCC · ULTCC · EMI Shielding · Composites · Rubber-Ceramics · PCBs · Dielectric Resonators · Microstrip antenna · Dielectric Resonator Antenna · Bandwidth · Metamaterials · Oscillator · Filter · Reflection Coefficient Gain · Beamwidth

**Abbreviations**

| | |
|---|---|
| 5G | Fifth generation |
| AESA | Active electronically steered antennas |
| BoPET | Biaxially oriented poly-ethylene terephthalate |
| BSE | Bore sight errors |
| CTE | Coefficients of thermal expansion |
| DR | Dielectric resonator |
| DRA | Dielectric resonator antenna |
| DRO | Dielectric resonator oscillator |
| EBG | Electromagnetic bandgap |
| ECM | Electronic countermeasures |
| EMI | Electromagnetic interference |
| EMP | Electromagnetic pulse |
| ESD | Electrostatic discharge |
| GPS | Global positioning systems |
| HARP | Halpern anti-radiation paint |
| HPSN | Hot-pressed silicon nitride |

| | |
|---|---|
| HTCC | High-temperature co-fired ceramics |
| HTPAHs | Heat-treated polyaromatic hydrocarbons |
| ICs | Integrated circuits |
| IoT | Internet of Things |
| IT | Information technology |
| ITS | Intelligent transport system |
| LTCC | Low-temperature co-fired ceramics |
| MCM | Multi-chip module |
| MCMB | Mesocarbon microbead |
| MICs | Microwave integrated circuits |
| MLC | Multilayer capacitor |
| MMICs | Monolithic microwave integrated circuits |
| MP | Melting point |
| MWCNT | Multiwall carbon nanotube |
| NRI | Negative refractive index |
| PCB | Printed circuit board |
| POE | Polyolefin elastomer |
| PPCP | Polypropylene random copolymer |
| PTFE | Polytetrafluoroeten |
| RBSN | Reaction-bonded silicon nitride |
| RF | Radio-frequency |
| RFI | Radio-frequency interference |
| RFID | Radio-frequency identification |
| SCFS | Slip-cast fused silica |
| SiP | System in package |
| SOP | System on package |
| TC | Thermal conductivity |
| UWB | Ultra-wideband |
| Wi-Fi | Wireless fidelity |
| WiMAX | Worldwide interoperability for microwave access |
| WLAN | Wireless local area network |

## Introduction

Microwave dielectric materials designed for wireless communication have been a booming area of growth. Microwave materials are fundamental building blocks for military and aerospace applications, which have been used as dielectric resonators, radomes, substrates, inks, multilayer packages, electromagnetic shield, etc. However, the stringent conditions and property requirements for the military and aerospace applications limit the availability of suitable materials. These materials and devices made of them should survive in harsh environmental conditions. Microwave materials can be used for signal propagation as well as shielding unwanted signals in defense and aerospace application depending on their properties. The properties which control the

material requirements for the signal propagation applications are very low relative permittivity to increase the signal speed; low dielectric loss to improve the selectivity as well as speed of the device; a low-temperature variation of relative permittivity/ resonant frequency for the reliable operation; and low coefficient of thermal expansion to prevent failure during the harsh environmental conditions. The materials used for these applications are in the form of bulk resonators; microwave substrates such as HTCC, LTCC, PCBs; etc. There is a growing demand for miniaturized and lightweight antennas with the reduction in the device size, platform, and budgets. The military and aerospace applications include different types of antennas such as microstrip antennas, dielectric resonator antennas, textile antenna, etc. Microwave materials, especially with dielectric constants of 2.2, 3.2, and 4.4, are used for the design of microwave filters as well as fractal antennas, ultra-wideband (UWB) antennas, reconfigurable microstrip antennas, etc. These antennas are suitable for modern communication systems (viz., Wi-Fi, WiMAX, Bluetooth, etc.). The microwave/millimeter-wave shielding materials are being used for EMI reduction, antenna pattern shaping, radar cross section and stealth technology. Presently, the demand for these EMI materials is increasing because of the growing number of warfare gadgets and space vehicles. Most of these applications used classified frequency ranges with integrated multiple antennas which need absorber materials to maintain the peak performance by reducing interference from nearby objects such as metal structures and other surrounded electronics. Electronic devices operating at high frequencies emit high-frequency noise which will cause resonance at specific frequencies when put inside the enclosure and hence hinder the device performance. Materials that are lossy (conductive/dielectric/magnetic loss) at these frequencies can attenuate the incoming electromagnetic interference. The present chapter gives an overview of microwave material requirements, properties, and their applications in antennas, filters, or oscillators in the defense and aerospace sector.

## Dielectric Resonators

A dielectric resonator is an electromagnetic device that exhibits resonance for a short range of frequencies. It is similar to that of a cylindrical metallic waveguide except that the boundary is defined by a substantial change in permittivity rather than by a conductor. Dielectric resonator (DR) is an unmetalled piece of the dielectric puck, which functions as a resonant cavity using reflections at the dielectric-air interface. The critical properties required for a dielectric resonator are low dielectric loss tangent (high-quality factor Q; $Q \sim 1/\tan \delta$), suitable relative permittivity ($\varepsilon_r$) (high permittivity for miniaturization and low permittivity for mm wave frequency communication and high-speed signal transmission), and near-zero temperature coefficient of resonant frequency ($\tau_f$). A dielectric resonator that satisfies all these three properties simultaneously is difficult to realize in a particular material. In the early microwave systems, bulk metallic cavities were used as resonators but were huge in size and not integrable with microwave integrated circuits (MICs). Although the stripline resonator is small and integrable in MIC, it has a poor quality factor with a poor temperature stability resulting in the instability of the circuit. Hence, the

importance of DRs, are due to easy integration in MICs with low loss and thermally stable frequency. DRs are important components for the manufacture of filters, oscillators, and antennas. They offer a size-reducing design alternative to bulky waveguide filters and low-cost alternatives for electronic oscillator frequency-selective limiter and antennas. The device performance is closely related to material properties. In addition to cost and size, other advantages that dielectric resonators possess over conventional metal cavity resonators are lower weight, material availability, and ease of manufacturing.

Richtmeyer theoretically predicted that a piece of dielectric with regular geometry and high $\varepsilon_r$ can confine electromagnetic energy within itself but still be prone to energy loss due to radiation [1]. It was found that through the total multiple internal reflections, a piece of the high $\varepsilon_r$ dielectric can confine microwave energy at a few discrete frequencies, provided the energy is fed in the appropriate direction. If the transverse dimensions of the sample are comparable to the wavelength of the microwave, then certain field distributions or modes will satisfy Maxwell's equations and boundary conditions. The reflection coefficient approaches unity as $\varepsilon_r$ approaches infinity. In the microwave frequency range, free space wavelength is in centimeters, and hence the wavelength inside the dielectric will be in millimeters only when the value of $\epsilon_r$ is in the range 20–100. To get resonance, dimensions of the dielectric must be of the same order (in millimeters). Still larger $\varepsilon_r$ gives higher confinement of energy, reduced radiation loss, and better miniaturization. However, high $\varepsilon_r$ will result in higher dielectric losses because of inherent material properties. The size of a DR is considerably smaller than the size of an empty resonant cavity operating at the same frequency, provided the relative permittivity ($\varepsilon_r$) of the material is substantially higher than unity. Higher $\varepsilon_r$ shrinks overall circuit/device size proportional to $1/(\varepsilon_r)^{1/2}$. For example, a circuit is compressed by a factor of six when a high Q ceramic with $\varepsilon_r = 36$ is substituted for a high Q air cavity $\varepsilon_r = 1$. The shape of a DR is usually a solid cylinder but can also be tubular, spherical, and parallelepiped. A commonly used resonant mode of a cylindrical DR is $TE_{01\delta}$.

At the resonant frequency, electromagnetic fields inside a resonator store energy equally in electric and magnetic fields. When $\varepsilon_r$ is about 40, more than 95% of the stored electrical energy and over 60% stored magnetic energy are located within the dielectric cylinder. The remaining energy is distributed in the air around the resonator, decaying rapidly with distance away from the resonator boundary. This is of great advantage since it enables one to couple microwave power easily to the DR by matching the field pattern of the coupling elements to that of the DR. The DR can be incorporated into a microwave network by exciting it with, e.g., microstrip transmission lines. The distance between the resonator and the microstrip conductor determines the amount of coupling. To prevent losses due to radiation, the entire device is usually enclosed in a metallic shielding box. High Q minimizes circuit insertion losses and can be used as a highly selective circuit. Besides, high Q suppresses the electrical noise in oscillator devices. When exposed to free space, a DR can also radiate microwave energy when it is fed suitably and can be used as efficient radiators, called dielectric resonator antennas (DRA).

The term dielectric resonator (DR) first appeared in 1939 when Richtmeyer showed that suitably shaped dielectric blocks could function as a microwave resonator; however, it took more than 20 years to generate further interest in DRs and to verify Richtmeyer's prediction experimentally. In the early 1960s, Okaya and Barash rediscovered DRs while working on rutile single crystals [2]. They measured the permittivity and Q of single crystals rutile at room temperature and down to 50 K in the microwave frequency range. In the early 1960s, Cohen and his co-workers performed extensive theoretical and experimental work on DRs [3]. Rutile ceramics that had an anisotropic permittivity of about 100 were used for their experiments, but rutile ($TiO_2$) has unfortunately, ($+450$ ppm/$^{\circ}$C) resonant frequency stability that prevented its commercial exploitation. The first microwave filter using $TiO_2$ ceramics was reported by Cohen in 1968, but it was not useful for applications because of its high $\varepsilon_r$ and frequency instability with temperature. A real breakthrough in dielectric resonator ceramic technology occurred in the early 1970s when the first temperature-stable low-loss barium tetra titanate ($BaTi_4O_9$) ceramic was developed by Masse et al. [4]. Later, barium nano-titanate ($Ba_2Ti_9O_{20}$) with the improved performance was reported by Bell Laboratories. The next breakthrough came from Japan when Murata Manufacturing Company produced $(Zr,Sn)TiO_4$ ceramics [5]. They offered adjustable compositions so that temperature coefficients could be varied between $+10$ and $-10$ ppm/$^{\circ}$C. Later, in 1975, Wakino et al. realized the miniaturization of the DR-based filters and oscillators [6]. Since then extensive theoretical and experimental work and development of several DR materials has occurred [7]. This early work resulted in the actual use of DRs as microwave components. Commercial production of DRs started in the early 1980s. About 4000 low-loss ceramic dielectrics are reported in the literature [8]. However, only a limited number of dielectric ceramic materials are useful for applications in the electronic industry. Especially ceramics with low permittivity are feasible for millimeter-wave communications and as substrates for microwave integrated circuits. The most common application area for the ceramics with medium permittivity in the range 25–50 is satellite communication and cell phone base stations. High-$\varepsilon_r$ materials are used in mobile phones where miniaturization of components is very important. For millimeter-wave applications, temperature-stable, low-permittivity, and high-$Q$ (low-loss) substrates are required for high-speed signal transmission with minimum attenuation. Table 1 gives a list of useful resonator materials for possible applications in space and defense. It may be noted that there are several factors such as porosity, grain boundaries, grain size, crystal defects, micro cracks, etc. that may affect the dielectric properties. For an ideal material, the main reason for the loss is due to the interaction of the microwaves with the phonons. One can tailor the properties of a particular material to some extent by suitable doping, substitution, additives, or mixture formation. The quality factor (Q) decreases with increasing frequency as shown in Fig. 1a, but the Qf remains nearly constant. However, smaller samples inherently contain less defects and shows higher Qf factor. The Qf decreases as temperature increases due to increase in lattice vibration. In general, the materials having high relative permittivity show a positive $\tau_f$ as

**Table 1** Shows some of the important DR materials useful for applications in space and defense [8].

| Material | Sintering temp | $\varepsilon_r$ | Qf GHz | $\tau_f$ |
|---|---|---|---|---|
| Fused silica | | 3.7 | 122,100 | – |
| $SiO_2$ | 1650 | 3.8 | 80,400 | −16 |
| (Cordierite) $Mg_2Al_4Si_5O_{18}$ + 7 wt.% $Yb_2O_3$ | 1420 | 4.9 | 112,500 | |
| $Li_2MgSiO_4$ + 1 wt% LBS | 925 | 5.5 | 114,300 | |
| Willemite ($Zn_2SiO_4$) | 1340 | 6.6 | 219,000 | −61 |
| $Mg_2SiO_4$ Fosterite | 1450 | 6.8 | 270,000 | −67 |
| $MgAl_2O_4$ | 1650 | 8.5 | 10,500 | −63 |
| $Zn_2SiO_4$ + 11 wt% $TiO_2$ | 1200 | 9.1 | 150,800 | −1 |
| $Al_2O_3$ | 1550 | 10.1 | 680,000 | −60 |
| $Mg_4Ta_2O_9$ | 1250 | 12.0 | 347,000 | −65 |
| $0.895Al_2O_3$–$0.105TiO_2$ | 1350 | 12.5 | 340,000 | 2 |
| $0.83ZnA_{l2}O_4$–$0.17TiO_2$ | 1410 | 12.6 | 100,200 | 0 |
| $MgTiO_3$ | 1350 | 16.1 | 289,400 | −54 |
| $0.94(Mg_{0.95}Zn_{0.05})_2TiO_4$–$0.06SrTiO_3$ | 1270 | 18.0 | 125,600 | 0 |
| $0.77(0.5ZnAl_2O_4$–$0.5TiO_2)$–$0.23MgTiO_3$ | 1390 | 18.7 | 190,000 | −2 |
| $0.96$ mg$(Zr_{0.05}Ti_{0.95})O_3$–$0.04SrTiO_3$ | | 20.8 | 257,000 | 0 |
| $Ba(Mg_{1/3}Ta_{1/3})O_3$ | 1650 | 25.0 | 430,000 | 0 |
| $Ba(Zn_{1/3}Ta_{2/3})O_3$ | | 28.0 | 168,000 | 1 |
| $Ba(Zn_{1/3}Ta_{2/3})O_3$ + 1 wt% $V_2O_3$ | 1600 | 28.4 | 236,000 | 0 |
| $0.7Ba(Co_{1/3}Nb_{2/3})O_3$–$0.3Ba(Zn_{1/3}Nb_{2/3})O_3$ | 1400 | 34.5 | 97,000 | 0 |
| $Ba_2Ti_9O_{20}$ | | 37.0 | 57,000 | 0 |
| $.95Ba(Zn_{1/3}Nb_{2/3})O_3$–$0.05Ba(Ga_{1/2}Ta_{1/2})O_3$ | | 38.0 | 102,900 | 19 |
| $Zn_{0.95}Co_{0.05}Ta_2O_6$ | | 38.5 | 112,000 | 11 |
| $(Zr_{0.8}Sn_{0.2})TiO_4$ | | 40.0 | 53,000 | 0 |
| $0.4LaAlO_3$–$0.6SrTiO_3$ | 1680 | 42.1 | 83,000 | 8 |
| $Bi_{12}SiO_{20}$ | 800 | 43.0 | 86,800 | −10 |
| $0.7CaTiO_3$–$03NdAlO_3$ | 1450 | 45.0 | 44,000 | 0 |
| $0.4ZnNb_2O_6$–$0.6TiO_2$ | 1125 | 46.2 | 48,000 | −1 |
| $0.66CaTiO_3$–$0.34(La_{0.5}Nd_{0.5})$ $GaO_3$ | 1540 | 49.0 | 43,000 | 0 |
| $0.48Nd(Zn_{1/2}Ti_{1/2})O_3$–$0.52SrTiO_3$ | 1350 | 54.2 | 84,000 | 0 |
| $CaTi_{0.7}(Al_{1/2}Nb_{1/2})_{0.3}O_3$ | 1450 | 65.4 | 19,300 | −2 |
| $Ba_{(2-x)}Sm_{(4 + 2/3x)}Ti_9O_{28}$ (x = 0.2) | 1370 | 74.8 | 10,900 | 2 |
| $Ba_{6-3x}Sm_{8 + 2x}Ti_{18}O_{54}$ | 1300 | 91.0 | 11,000 | 3 |
| $TiO_2$ + 0.05 Mol% $Fe_2O_3$ | 1500 | 102.0 | 50,100 | 400 |
| $Sr_3Ce_2Ti_6O_{19}$ ($Sr_{1−3x/2}Ce_xTiO_3$ x = 0.333) | 1350 | 123.0 | 10,000 | 392 |

shown in Fig. 1b. The resonant frequency of the sample depends on the relative permittivity and dimensions. The higher the permittivity, the smaller the resonant frequency and higher dimensions give smaller resonant frequency. Hence, for very high-frequency applications such as mm-wave applications, materials with lower permittivity and smaller dimensions are required.

**Fig. 1** Plot of (**a**) Qf and (**b**) $\tau_f$ versus permittivity
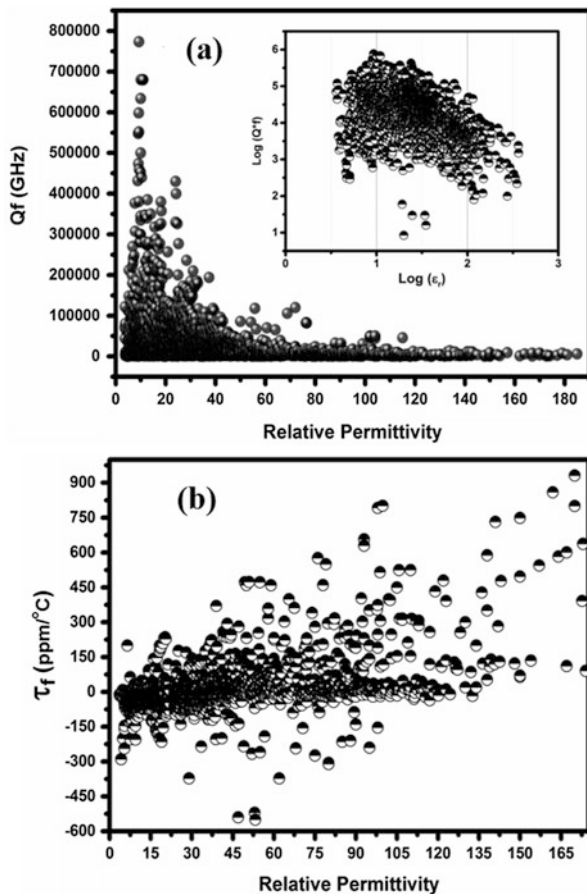


# Ceramic Substrates/Packages and Inks for Military and Aerospace Applications

The military and aerospace sector is one of the fastest-growing industries in the world. The rapid growth in military and aerospace telecommunication applications requires precise device performance, which is one of the extremely important factors as compared to the general telecommunication applications. Most of the military and aerospace equipment are working in the most hostile areas of the earth and in challenging environments such as battlefields, on land, under water, and in air. Most of these specific applications are in the microwave/millimeter-wave frequency ranges. Hence, high-quality ceramic substrate/packages with good thermal and mechanical stability along with excellent microwave/millimeter-wave dielectric properties are commonly required for these applications. IBM first utilized a multi-chip module (MCM) in its high-end system 370 in the early 1980s. Later on, 50 mm
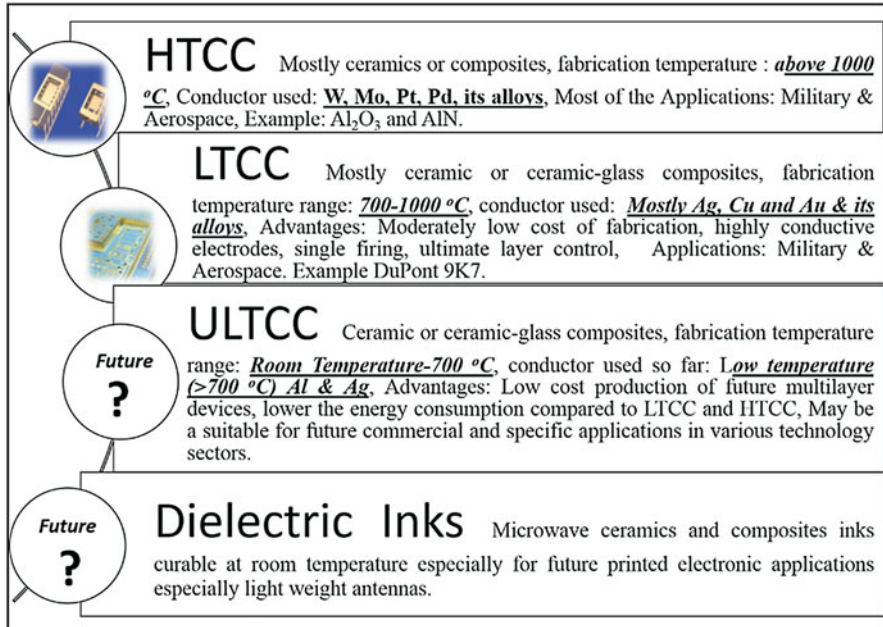
**Fig. 2** Past, present, and future trends of ceramic processing technology

square, nine-chip MCM replaced 700 of the previous generation module. Multilayer capacitor (MLC) products are still made today in the same way as the original RCA products of the 1950s and 1960s [9–11]. From a historical perspective, guided electromagnetic wave propagation in dielectric media received much attention in the early days of microwave research.

Later, the technological growth demanded high-temperature co-fired ceramics (HTCC), low-temperature co-fired ceramics (LTCC), ultralow temperature ceramics (ULTCC), and very recently inks/paints [7, 12]. Among these ceramic processing technologies, HTCC and LTCC substrate or packages are the key products of air traffic, defense, and space applications. However, ULTCC and ceramic inks are in the growing stage of research for these application areas. In this section, we discuss the commercially useful and suitable HTCC, LTCC, and ULTCC substrates/packages and dielectric inks for military and aerospace applications such as active electronically steered antennas (AESA) with hundreds or even thousands of T/R modules operating in different platforms and systems [13, 14]. Figure 2 shows the past, present, and future trends of ceramic processing based on the ceramic technology growth.

## HTCC and LTCC Substrate/Packages

The HTCC (fabrication temperature above 1000 $^{\circ}$C)/LTCC (fabrication temperature ranges 700–1000 $^{\circ}$C) materials used as microwave substrates or packages in

microelectronic devices especially in the harsh environments should fulfil diverse requirements like low dielectric loss, low relative permittivity, good temperature stability, high thermal conductivity, and low coefficient of thermal expansion [7, 12]. Low relative permittivity minimizes capacitive coupling as well as signal delay, and low dielectric loss tangent reduces signal attenuation along with better device performance [15]. The most common electrode materials used for co-firing the HTCC and LTCC are W (MP: 3410 °C), Mo (MP: 2610 °C), Pt (MP: 1769 °C), Pd (MP: 1552 °C), Cu (MP: 1083 °C), Au (MP: 1063 °C), and Ag (MP: 961 °C) and their alloys due to the desired electrical conductivity, fabrication temperature, and integration compatibility or reactivity with HTCC/LTCC materials [7]. The dielectric materials as HTCC/LTCC substrates or packages contribute essential control over a wide range of electrical and microelectronic device applications utilized in high-temperature environment.

Most commonly used HTCC substrate and packaging material is $Al_2O_3$ due to its low-cost superior thermal, mechanical, and electrical properties. The alumina substrate and packages have been extensively used in microelectronic packages for decades especially in the military and aerospace sector. Military and aerospace systems utilize the current transceiver manufacturing approach and are based on ceramic packages (either HTCC or LTCC) [7, 12, 16]. This can be achieved by fulfilling the following conditions such as (a) meeting the high performance specifications of the applications, (b) scalability in terms of circuit density and power density characteristics, (c) compatibility with low-volume military and aerospace assembly facilities, and (d) compatibility with existing infrastructures [17]. There are large numbers of materials reported in the literatures for HTCC and LTCC applications [7, 17]. However, in the last two decades, $Al_2O_3$-based HTCC substrate/packages are mostly employed in the military and aerospace sector especially for microwave telecommunications. The raw material of HTCC alumina for these specific applications is different from general-purpose HTCC alumina, and more importantly, there is no glass additive in this alumina material for co-firing processes [17]. Chen et al. reported that a high-temperature co-fired ceramic (HTCC) alumina material improved dielectric performance at high temperatures as compared with the 96% alumina substrate suggesting its potential use for high-temperature packaging applications. Moreover, they demonstrated a prototype 32-I/O (input/output) HTCC alumina package with platinum conductor for 500 °C low-power silicon carbide (SiC)-integrated circuits, and such devices are currently under development for aerospace applications [18]. These hard ceramics have plethora of applications in military, aerospace, medical devices, and telecommunications. Hard ceramic substrates and package are widely used for multi-chip module (MCM) and monolithic microwave integrated circuits (MMICs) used in high-temperature environment [19, 20]. Recently, Varghese et al. reported natural zircon ($ZrSiO_4$)-based HTCC substrate which has good and comparable thermal, mechanical, and dielectric properties as that of commercial $Al_2O_3$ HTCC substrates. Figure 3 shows the (a) photograph of $ZrSiO_4$ sand, (b) cast green tape of processed $ZrSiO_4$, inset shows the microstructure of green cast tape, and (c) sintered $ZrSiO_4$ HTCC substrate, inset shows the microstructure of sintered substrate at 1600 °C [21, 22]. The detailed thermal, mechanical, and dielectric properties are shown in Table 2 [23–27]. More recently Roshni et al. reported
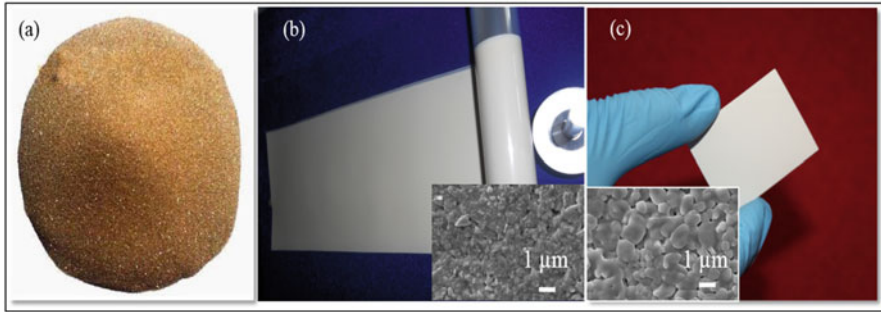
**Fig. 3** (**a**) photograph of $ZrSiO_4$ sand, (**b**) cast green tape of processed $ZrSiO_4$, inset shows the microstructure of green cast tape, and (**c**) sintered $ZrSiO_4$ HTCC substrate, inset shows the microstructure of sintered substrate at 1600 °C. (Source: Adapted from [12])

**Table 2** Commercial and suitable reported HTCC/LTCC substrates or packages for military and aerospace applications [7, 23–27]

| Substrates or packages (electrodes) | Microwave dielectric properties (>5 GHz) | | Thermal properties | | Mechanical properties | |
|---|---|---|---|---|---|---|
| | $\varepsilon_r$ | tan$\delta$ $(10^{-4})$ | TC Wm$^{-1}$ K$^{-1}$ | CTE (ppm/°C) | Hardness (Moh's) | FS (MPa) |
| $Al_2O_3$ 96% (W, Mo, CuW) | 9.5–9.9 | 1–4 | 25–35 | 6–8 | 9.0 | 450–650 |
| $ZrSiO_4$ (Pt) | 9.2 | 3 | 15 | −2.5 | 6.5–7.5 | 150–200 |
| AlN (W) | 8.6 | 170 | 200–230 | 4.2–5.8 | 7.0 | 300–450 |
| $0.83ZnAl_2O_4$–$0.17TiO_2$ | 9.6 | 8 | 31.3 | 6.59 | 7–8 | – |
| DuPont 9 K7 | 7.1 | 10 | 4.6 | 4.4 | 5–6 | 230 |
| DuPont 951 | 7.8 | 100 | 3.3 | 5.8 | 5–6 | 320 |
| Ferro A6M | 5.7 | 20 | 2 | 7 | 6 | 170 |
| Kyocera GL330 | 7.7 | 5 | 4.3 | 8.2 | 9 | 400 |
| Kyocera GL570 | 5.7 | 7 | 3.4 | 2.8 | 6.5 | 200 |
| NTK NOC | 5.9 | 6 | 3 | 5.2 | 6.5 | 250 |
| NTK GM-1 | 6.5 | 20 | 2 | 3.5 | 6.5 | 250 |
| $Li_2ZnTi_3O_8$−1wt.% LMZBS | 21.3 | 7 | 5.8 | 11.97 | – | – |
| $Bi_4(SiO_4)_3$ | 13.3 | 7 | 2.82 | 7.9 | – | – |
| $LiMgPO_4$ | 6.4 | 2 | 7.1 | 10.5 | | |

yet another alternative HTCC substrate based on zinc aluminate-titania with better thermal conductivity than alumina [28]. Table 2 also represents the common and suitable HTCC/LTCC package properties for military and aerospace applications. HTCC substrates such as aluminum nitride (AlN) and beryllium oxide (BeO) are also used in some specific applications due to their high thermal conducting (TC) properties such as

TC > 200 $Wm^{-1} K^{-1}$ and TC > 100 $Wm^{-1} K^{-1}$ [28]. Kaneko et al. reported a comparative study of various HTCC substrates such as AlN, ceramic-glass, and alumina with different electrodes such as Ti(0.008mil)/Cu(0.08mil)/Ni(0.04mil)/Au (0.08mil) [29]. In the MW studies, AlN-based HTCC multichip module (MCM) shows good electrical performance and high reliability due to good thermal management, matching CTE, and the hermeticity with extremely simplified structure suitable for mass production [29]. For many envisioned applications such as military and aerospace, operational durability is a critical factor. There are also several reports on SiC-based HTCC JFET ICs which exhibits prolonged (>10,000 h) durability, stability, and reliability near 500 °C similar to $Al_2O_3$ and AlN [30, 31]. The HTCC are mainly used for Quad Flat No-lead (QFN) package. These packages from Barry Industries have low-loss broadband transitions with a superior performance over frequency of about 40 GHz. Important benefits of HTCC constructions against the LTCC ones are enhanced mechanical strength and higher thermal conductivity [32].

In comparison with HTCC, LTCC substrates are the present generation low-cost multilayer technology with fabrication temperature in the range of 700–1000 °C. In this technology, highly conductive Ag, Cu, and Au electrodes are widely used for co-firing purpose. In addition to this, ceramic-glass and glass-free LTCC substrates are also reported to have wide range of applications especially in the military and aerospace telecommunications. From manufacturing aspects, the system-in-package (SiP) integration solution offers the best balance between cost and performance to satisfy the demands of these different applications. So far, the state-of-the-art demonstrators have been accomplished in LTCC substrates. On the other hand, millimeter-wave antennas and arrays with wideband and high integration are receiving increasing demand in aerospace and military applications.

The LTCC technology is a good option for integration at mm-wave because of lightweight, low profile, compactness, easy integration, and excellent high-frequency performance. Moreover, most of these applications required high routing density, low dielectric losses, cost-effective interconnects, and packaging solutions. LTCC technology combines these characteristics, making it as a well-suited System On Package (SOP) and densely populated multichip modules (MCM). Commonly used commercial LTCC for high-frequency (up to 100 GHz and beyond) applications are DuPont 9 k7. It has permittivity of 7.1 and dielectric loss of 0.001 reported at 10 GHz. Moreover, 9 k7 has X, Y shrinkage of 9.1% and Z shrinkage of 11.8% along with flexural strength of 230 MPa, thermal conductivity of 4.6 W/mK, coefficient of thermal expansion (CTE) of 4.4 ppm/°C, and surface roughness of 0.52 μm [33, 34]. Another low permittivity LTCC tape from Ferro Corporation, A6M (material unknown, firing temperature 450–850 °C) has permittivity of 5.9 and dielectric loss of 0.002 at (1–100 GHz), along with X, Y shrinkage of 15. 4% and Z shrinkage of 28%. It has CTE of 7 ppm/°C, thermal conductivity of 2 W/m.K, flexural strength of 170 MPa, and surface roughness of 0.9 μm [25]. Recently Varghese et al. reported that indialite/cordierite-$Bi_2O_3$ LTCC with relative permittivity of 6 and dielectric loss of 0.0001 when fired at 900 °C is a potential candidate for applications [21]. This composite has less than 20% X, Y and Z shrinkages and are shown in Fig. 4.
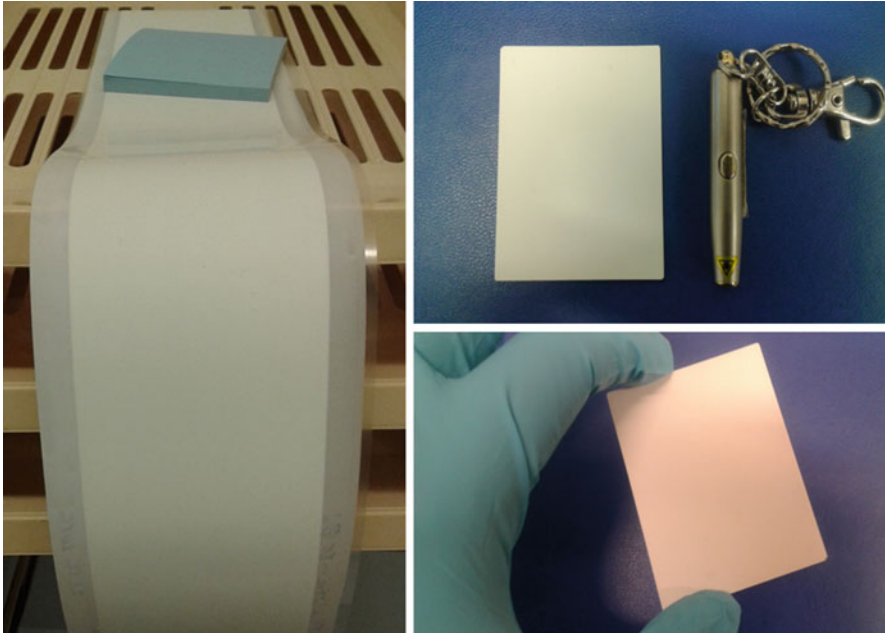
**Fig. 4** Low permittivity and low dielectric loss LTCC system based on indialite-$Bi_2O_3$. (Adapted from [21])

## Ultralow Temperature Co-Fired Ceramic Packages

Ultralow temperature co-fired ceramic (ULTCC) technology is a new promising ceramic technology based on the concept of HTCC and LTCC. The ULTCC research is in the rudimental stage for applications in the commercial as well as military and aerospace sectors. It brings down the fabrication temperature below 700 °C and mostly co-firable with Al or Ag or its alloys. Recent review by Sebastian et al. forecasted the materials research strategy for future ULTCC-based devices [7].

Based on the review, there are few materials, which are suitable for the military and aerospace applications such as substrates for antennas and other packaging and embedded devices such as capacitors and resistors [7]. Table 3 presents a few ULTCC materials which may be suitable for future military- and aerospace-based substrate and packaging solutions based on their dielectric properties at microwave frequency [35] ranges. It is clear from Table 3 that only a very few materials are reported to have highest Qf which are suitable for high-frequency applications especially military and aerospace sectors. The temperature coefficient of resonant frequency is also one of the key requirement for these applications. Still more research such as co-firability and thermal and mechanical properties needs to be done for ULTCC to reach real applications to meet the stringent requirements of military and aerospace sectors.

**Table 3** List of possible materials for future ULTCC substrate/packaging applications [35–39]

| Materials (ULTCC) | Sintering temperature | Microwave dielectric properties at > 5 GHz | | Electrode compactability |
|---|---|---|---|---|
| | | $\varepsilon_r$ | Qf | |
| $Li_2Ca_2Mo_3O_{12}$ | 630 | 8.5 | 108,000 | Not for Ag and Al |
| $CaV_2O_6$ | 675 | 10.2 | 123,000 | Not studied |
| $Li_2CeO_3$ | 690 | 11.2 | 100,000 | Yes for Al |
| $Ba_{16}V_{18}O_{61}$ | 620 | 9.7 | 80,100 | Yes for Ag |
| $Sr_{16}V_{18}O_{61}$ | 660 | 9.8 | 75,600 | Yes for Ag |
| $Ca_{16}V_{18}O_{61}$ | 680 | 11.1 | 79,100 | Yes for Ag |
| $Li_2Zn_2Mo_3O_{12}$ | 630 | 11.1 | 70,000 | Yes for Ag, Al |
| $Zn_2Te_3O_8$ | 610 | 14.2 | 70,100 | |
| $Li_2WO_4$ | 640 | 5.5 | 62,000 | Not for Ag, yes for Al |
| $MgTe_2O_5$ | 700 | 10.5 | 61,000 | Not studied |
| $Sm_2Mo_4O_{15}$ | 690 | 10.7 | 63,500 | Yes for Ag |
| $Nd_4Mo_4O_{15}$ | 700 | 11.1 | 61,500 | Yes for Ag |
| $Zn_2Te_3O_8$ + 10 wt% $TiTe_3O_8$ | 600 | 16.5 | 65,400 | Yes for Al |
| $CuMoO_4$ | 650 | 7.9 | 53,000 | Yes for Al |
| $CuMoO_4-Ag_2O_3$ | 500 | 8.3 | 32,000 | Yes for Al |
| $TiO_2$-GO17 | 400 | 15.5 | 3300 | Yes for Ag |

## Dielectric Inks/Paints

Microwave dielectric ink research has been getting increasing interest in the recent years for focusing the low-density applications like printed electronics. The ultimate goal of this research is to develop highly efficient lightweight portable devices, which may have good demand in the military and aerospace sectors in the near future. The research in this area is expanding to explore the low permittivity and low dielectric loss dielectric ink even at room temperature. Varghese et al. reported the first room temperature curable dielectric $SiO_2$ ink printed on commercial BoPET film with relative permittivity of 2.4–2.3 and dielectric loss of 0.003–0.006 in the frequency range of 8–18 GHz [7]. The $ZrSiO_4$ ink deposited on BoPET shows relative permittivity of 3.4–3.3 and dielectric loss of 0.003–0.004 in the X and Ku band frequency ranges [7]. Table 4 gives the microwave dielectric properties of room temperature curable as well as sintered dielectric ink which may find applications in military and aerospace especially printed dielectric antennas. The dielectric ink research is still in the rudimental stage for processing as well as device level testing.

**Table 4** Room temperature curable dielectric ink suitable for microwave applications [40–45]

| Dielectric inks | Microwave dielectric properties at >5 GHz | |
| --- | --- | --- |
| | $\varepsilon_r$ | $\tan\delta$ |
| $SiO_2$ on BoPET | 2.4–2.3 | 0.003–0.006 |
| $ZrSiO_4$ on BoPET | 3.4–3.3 | 0.003–0.004 |
| $Al_2O_3$ on BoPET | 2.9 | 0.004 |
| $Bi_2MoO_2$ on $Al_2O_3$ substrate | 35 | 0.001 |
| Boron nitride on BoPET | 1.9 | 0.01 |
| Nano $Bi_4(SiO_4)_3$ on BoPET | 4.2 | 0.01 |

## Polymer-Ceramic Composites for Microwave Substrate Applications

Polymer-ceramic composites, especially type 0–3, are a potential group of materials suitable for functional packages, which combine the electrical properties of ceramics and the mechanical flexibility, chemical stability, and processing features of polymers. The important characteristics required for microwave substrates for packaging technology are high-frequency compatibility, low dielectric losses, moderate dielectric constant, low coefficient of thermal expansion, high thermal conductivity, low-temperature variation of relative permittivity, low or no moisture absorption, and high dimensional stability. The dielectric loss tangent of base dielectric substrates are not so critical while designing circuits below 1 GHz. Hence, comparatively low dielectric loss tangent PCB materials made from epoxy/woven fabric composites are often used as base substrates. However, as the operational frequencies exceed 1 GHz, the dissipative signal loss in the substrate becomes more significant, and the $\tan\delta$ parameter of the substrate cannot be ignored. The $\varepsilon_r$ value of the substrate material also has a profound influence on signal propagation, as the speed of the signal passing through the dielectric medium is inversely proportional to the square root of $\varepsilon_r$. Thus, the choice of the substrate material becomes very important at the designing stage of a microwave circuit for various electronic devices used in defense, space, and information technology (IT). Presently, the microwave component industry uses several substrate materials comprising hard and soft substrates. The ceramic substrates have the advantage of withstanding the localized heat caused during the wire-bonding process. In general, the hard ceramic substrates are highly isotropic with high operating temperature along with high thermal conductivity ($k$), low CTE, low or high permittivity and low dielectric loss. However, they exhibit brittleness, difficulty in machining, and a relatively high cost of chemically and thermally compatible conducting layer. The polymers have a low dielectric constant and low loss tangent but a high CTE, high-temperature variation of relative permittivity $\tau\varepsilon$, very low thermal conductivity, and good mechanical properties. Hence, by using the composite approach, one can get reasonably good properties

for practical applications in microelectronics. The soft polymer-ceramic substrates made out of both thermoset plastic and thermoplastic materials generally have good machinability, better shock resistance, a low-cost conduction/metallization layer, tailor-made properties, and useful electrical properties.

It is well known that connectivity between the phases in the composite materials is very important in achieving the desired properties. The interspatial relationships in a multiphase material, the connectivity, control the mechanical and electrical properties and thermal fluxes between the phases. The ceramic filler particle size, shape, interfacial properties, percolation level, and porosity play a crucial role on the properties of the composite [7, 46]. Polymer matrix composites can be classified into two categories depending on the nature of the matrix used, i.e., thermoset or thermoplastic. Thermoplastic materials have a melt temperature associated with them, whereas dimensional behavior of thermosets is characterized by its glass transition temperature ($Tg$). Among them, thermoset matrix composites are most preferred for low-end applications, whereas thermoplastic composites are the material of choice. for high-end microwave circuit applications. The main advantages of thermoplastic matrix composites compared with thermoset matrix composites are an unlimited shelf life and does not require curing, reprocess ability, chemical inertness, lower moisture absorption, higher service temperature, and high environmental tolerance. However, the processing difficulties and relatively high viscosity are some drawbacks of thermoplastic materials. Most common base substrate used for microwave circuit fabrication is the epoxy/glass substrate (FR-4) having a relative permittivity of 4.4 with loss tangent of 0.05 at 800 MHz. FR-4 is fabricated through hot pressing of woven fabric/brominated epoxy composites [47]. However, the use of FR-4 substrates at high frequencies (>1 GHz) is restricted due to their higher loss tangent [48]. Several materials based on thermosetting polymer matrix are available for high-frequency applications [7, 49]. One of the most common PCBs for high-frequency application is filled poly(1,2-butadiene) composites [50]. These composites exhibit a low porosity content even at a filler loading of 60 vol.%. Poly (1,2-butadiene)-based substrates have dielectric constants of 3.27, 4.5, 6, 9.2, and 9.8 with a loss tangent <0.0025 at 10 GHz and are commercially available. Table 5 shows the properties of some of the poly(1,2-butadiene)-based high-frequency substrate materials (TMM of Rogers corporation) that are commercially available. Laminates based on thermoset polymers need only ordinary processing techniques but suffer from a high moisture absorption content and low tensile strength. Long-term exposure of these thermoset matrix substrates to a highly oxidative environment may lead to change in the dielectric properties of hydrocarbons and hence the substrates. It is difficult to use this class of materials in an extreme chemical environment [51].

Thermoplastic materials compared to the thermoset ones have higher chemical inertness and service temperature. Various thermoplastics having with low dielectric losses are used as the matrix in flexible microwave substrates. The research on polymer composites was mainly focused on thermoplastic polymers like polyimide, polydimethylsiloxane, polystyrene, polyethylene, benzocyclobutene, polymethyl methacrylate, metallocene cyclic olefin, polyphenylene sulfide, polyolefin elastomer

**Table 5** Ceramic-filled polymer composites [7, 46]

| Polymer | Filler | $V_f$ | $\varepsilon_r$ | tan$\delta$ |
|---|---|---|---|---|
| PTFE | $CeO_2$ | 0.6 | 5.0 | 0.0064 |
| PTFE | $SiO_2$ | 60 wt% | 2.9 | 0.0024 |
| PTFE | $ZnAl_2O_4$-$TiO_2$ | 0.6 | 4.8 | 0.008 |
| PTFE | $SrTiO_3$ | 63 wt% | 13.1 | 0.0055 |
| PTFE | $TiO_2$ | 0.67 | 10.2 | 0.022 |
| PTFE | $2MgO$-$2Al_2O_3$-$5SIO_2$ | 60 wt% | 3.2 | 0.0034 |
| PTFE | $Bi_2O_3$-$ZnO$-$Nb_2O_5$ | 0.6 | 12.5 | 0.001 |
| PTFE | $Al_2O_3$ | 0.66 | 4.3 | 0.0021 |
| PTFE | $MgO$ | 0.56 | 3.3 | 0.015 |
| PTFE | $CaTiO_3$ | | 11.8 | 0.0036 |
| PTFE | $BaNdSmTi_4O_{12}$ | 67 wt% | 8.0 | 0.009 |
| PTFE | $Sr_2Ce_2Ti_5O_{16}$ | 0.4 | 7.7 | 0.08 |
| PTFE | $MgTiO_3$ | 50 wt% | 4.3 | 0.0009 |
| PTFE | $CaTiO_3$ | 0.4 | 13 | 0.001 |
| PTFE | $TiO_2$/$SiO_2$ | 5 wt% / 50 wt% | 2.8 | 0.00075 |
| PTFE | $Sr_2ZnSi_2O_7$ | 0.5 | 4.4 | 0.003 |
| PTFE | $BaWO_4$ | 74 wt% | 4.3 | 0.004 |
| PTFE | BMT | 67 wt % | 6.7 | 0.0018 |
| PTFE | $TeO_2$ | 0.6 | 5.4 | 0.006 |
| PTFE | $Sm_2Si_2O_7$ | 0.4 | 3.9 | 0.0054 |
| PTFE | AlN | 0.5 | 4.2 | 0.006 |
| PTFE | $Mg_2SiO_4$ | 0.5 | 3.2 | 0.009 |
| Polyethylene | $Sm_2Si_2O_7$ | 0.4 | 4.8 | 0.0055 |
| Polyethylene | $Ca([Li_{1/3}Nb_{2/3}]_{0.8}Ti_{0.2}]O_3$ | 0.4 | 7.7 | 0.004 |
| Polyethylene | $Li_2MgSiO_4$ | 0.4 | 3.5 | 0.0032 |
| Polyethylene | $Sr_9Ce_2Ti_{12}O_{36}$ | 0.4 | 12.1 | 0.004 |
| Polystyrene | $Li_2MgSiO_4$ | 0.4 | 3.8 | 0.012 |
| Polystyrene | $Sm_2Si_2O_7$ | 0.4 | 4.34 | 0.0101 |
| Polystyrene | $Sr_2Ce_2Ti_5O_{15}$ | 0.5 | 13.6 | 0.0004 |
| Polystyrene | $Ca([Li_{1/3}Nb_{2/3}]_{0.8}Ti_{0.2}]O_3$ | 0.4 | 7.4 | 0.003 |
| Polystyrene | $Mg_2SiO_4$ | 0.5 | 4.0 | 0.006 |
| HDPE | $Sr_2Ce_2Ti_5O_{15}$ | 0.4 | 11.0 | 0.006 |
| HDPE | $Ca_4La_6(SiO_4)_4(PO_4)_2O_2$ | 0.4 | 5.1 | 0.0023 |
| HDPE | $CeO_2$ | 0.4 | 11.0 | 0.006 |
| HDPE | $Mg_{0.95}Ca_{0.05}TiO_3$ | 0.5 | 7.32 | 0.001 |
| HDPE | $Li_2MgSiO_4$ | 0.4 | 3.54 | 0.0032 |
| HDPE | $Sm_2Si_2O_7$ | 0.5 | 5.3 | 0.009 |
| HDPE | $ZrSiO_4$ | 0.4 | 4.8 | 0.0018 |
| POE | $SrTiO_3$ | 0.4 | 11.0 | 0.010 |
| POE | $SrTiO_3$-NiZn ferrite | | 5.4 | 0.0018 |
| PEEK | $TiO_2$ | 25 wt% | 4.9 | 0.0087 |

(continued)

**Table 5**  (continued)

| Polymer | Filler | $V_f$ | $\varepsilon_r$ | tan$\delta$ |
|---|---|---|---|---|
| PEEK | $SrTiO_3$ | 27 wt% | 5.2 | 0.003 |
| Poly(methyl methacrylate) | $Ba_{0.6}Sr_{0.4}TiO_3$ | 0.416 | 1212 | 0.026 |
| Metallocene cyclic olefin copolymer | Soda lime borosilicate | 0.36 | 1.92 | 0.0009 |
| Cyclo-olefin polymer | MgO | 0.3 | 3.8 | 0.0005 |
| COC | BST | 0.25 | 6.0 | 0.0023 |
| Polyphenylene sulfide (PPS) | BST | 0.7 | 13.5 | 0.0025 |
| PPS | Mica/$SrTiO_3$ | 0.38 | 6.4 | 0.0052 |
| PPS | Mica/$SrTiO_3$ | 14 | 6.4 | 0.0053 |
| Polyimide | $BaTiO_3$ | 0.1 | 35.0 | 0.0082 |
| LCP | – | – | 3.0 | 0.002 |
| DGEBA | $Mg_2SiO_4$ | 0.4 | 3.8 | 0.014 |
| Epoxy | $Sr_9Ce_2Ti_{12}O_{36}$ | 0.4 | 14.1 | 0.022 |
| Epoxy | PMN-PT/$BaTiO_3$(3:1) | 0.7 | 89.0 | 0.017 |
| Epoxy | $BaTiO_3$ | 0.6 | 45.0 | 0.035 |
| Epoxy | $BaTiO_3$ | 0.45 | 13.1 | 0.025 |
| Epoxy | PMN-PT-$BaTiO_3$ | 0.7 | 110.0 | 0.016 |
| Epoxy | Ca(Li,Nb,Ti)$O_3$ | 0.3 | 8.0 | 0.009 |
| Epoxy | Ca(Li, Nb,Ti)$O_3$-Ag | 0.26 Ag | 72.3 | 0.065 |
| Epoxy | $(Ba_{0.9}Sr_{0.1})(Ti_{0.9}Zr_{0.1})O_3$ | 70 wt% | 25.2 | 0.035 |
| Polypropylene | $Zn_2SiO_4$ | 0.335 | 2.9 | 0.00018 |
| Polypropylene | $MgAl_2O_4$ | 0.2 | 3.0 | 0.00017 |
| RT duroid 6010 LM | PTFE – ceramic | – | 10.2 | 0.0018 |
| RT duroid 5870 | PTFE – glass microfibers | – | 2.3 | 0.0023 |
| RT duroid 6002 | | – | 2.9 | 0.0012 |
| RO 4533 | | | 3.3 | 0.0020 |
| RO 4534 | | | 3.4 | 0.0022 |
| RO 4535 | | | 3.5 | 0.0032 |
| RO 4350 | | | 3.4 | 0.004 |
| FR4 | Fiberglass-reinforced epoxy | | 4.2 | 0.020 |
| TFG | | | 3.2 | 0.003 |
| TPG30 | | | 2.8 | 0.0027 |
| TLG-29,TLG-30, TLG-32, TLG-33, TLG-34,TLG-35 | | | 2.8–3.5 | 0.0024–0.0029 |
| TLT | PTFE-fiberglass fabric | | 2.5 | 0.0006 |
| TLP | PTFE-fiberglass fabric | | 2.1 | 0.0009 |
| TLC | | | 2.7–3.20 | 0.0030 |
| TLE | | | 2.9–3.00 | 0.0028 |
| RF-35 | | | 3.5 | 0.0028 |
| RF-35P | | | 3.5 | 0.0035 |
| TSM-30 | | | 2.9 | 0.0012 |

<div align="right">(continued)</div>

**Table 5** (continued)

| Polymer | Filler | $V_f$ | $\varepsilon_r$ | $\tan\delta$ |
|---|---|---|---|---|
| TLY | PTFE woven glass | | 2.1–2.4 | 0.0009 |
| TLX | PTFE woven glass | | 2.4–2.6 | 0.0019 |
| Taclamplus | | | 2.1 | 0.0004 |
| RF-60A | | | 6.1 | 0.0038 |
| RF-41,RF-43,RF-45 | | | 4.1–4.5 | 0.0033–0.0038 |
| TRF -41,TRF-43,TRF-45 | PTFE woven glass reinforced | | 4.1–4.5 | 0.0035 |
| RF-30 | | | 3.0 | 0.0014 |
| HyRelex | | | 2.6 | 0.0020 |
| Cr-10 | | | 10.0 | 0.0035 |
| Arlon 25FR and 25 N | | | 3.3 | 0.0025 |
| FASTRISE 27 | | | 2.7 | 0.0020 |
| TSM29 | | | 2.9 | 0.0014 |
| CLTE | | | 2.9–3.0 | 0.0012–0.0023 |
| TC350 | | | 3.5 | 0.0020 |
| TC600 | | | 6.1 | 0.0020 |
| AD255A,AD260, AD300A,AD320A, AD350A,AD410A, AD430A | | | 2.5–4.3 | 0.0015–0.0035 |
| AD1000A | | | 10.2 | 0.0023 |
| AD600 | | | 6.0 | 0.003 |
| AR1000 | | | 9.8 | 0.003 |
| 25 N | | | 3.3 | 0.0025 |
| 25FR | | | 3.5 | 0.0035 |
| DiClad 880-PIM | | | 2.1 | 0.0009 |
| IsoClad 917 | | | 2.1 | 0.0013 |
| CuClad 250 GT | | | 2.4 | 0.001 |
| Nelco N4000–13 | | | 3.7 | 0.008 |
| Nelco 4000–13 SI | | | 3.4 | 0.008 |
| Nelco 400013SI | | | 3.3 | 0.007 |
| TMM3[a] | | | 3.2 | 0.002 |
| TMM4[a] | | | 4.5 | 0.002 |
| TMM6[a] | | | 6.0 | 0.0022 |
| TMM10[a] | | | 9.2 | 0.0023 |
| TMM10i[a] | | | 9.8 | 0.002 |

[a]TMM is the registered trademark of poly (1, 2-butadiene)-based substrates by M/s. Rogers Corporation, USA

(POE), polypropylene, and polyurethane copolymers. In these composites, the polymers are commonly reinforced with glass or ceramic. PTFE is also the most preferred host matrix due to its excellent dielectric properties such as low permittivity and extremely low loss tangent, and it is very stable in a wide frequency range.

The properties of PTFE such as chemical inertness, low moisture absorption, high service temperatures, etc. are also important for many microwave applications. All the reported polymer-ceramic composites show an increase in loss tangent with increasing frequency. Recently Krupka et al. found that polypropylene-silicon composites show a decrease in loss tangent with increasing frequency and propose it as a useful composite for 5G and IoT which operate at very high frequencies [52]. Table 5 gives a list of polymer-ceramic composites useful for practical applications like electronic packages for device encapsulation protecting them from an adverse environment and increasing their long-term reliability. The electrical characteristics of microelectronic devices, such as signal attenuation, propagation velocity, and cross talk, are influenced by the dielectric properties of the packaging materials. An important role of the packaging materials is to ensure the electrical insulation of the silicon chip and circuit pins. A low conductivity is needed to avoid leakage current, a low $\varepsilon_r$ to minimize the capacitive coupling effects, and a low loss factor to reduce signal loss.

The 0–3 type polymer-ceramic composites offer an opportunity to manufacture materials combining the electrical and mechanical properties of both polymers and ceramics. A composite with three-dimensionally connected polymer phase loaded with isolated ceramic particles (0–3 connectivity) finds extensive applications in microelectronic industry. One of the biggest advantages is the possibility of adjusting the electrical, thermal, and mechanical properties continuously as a function of ceramic loading, enabling unique freedom to component designers. The relative permittivity and thermal conductivity increase with ceramic loading, whereas the CTE decreases. The loss tangent in general increases with ceramic loading. The dielectric properties are mainly dependent on the polymer matrix until the level of the percolation limit. Usually the filler addition is limited to about 50–60 volume fraction. Preparation of composites with a larger volume fraction of filler (more than 50–60) is difficult, and the amount of porosity increases.

The polymer-ceramic composites facilitate the fabrication of inexpensive and very complex three-dimensional (3D) structures. This offers a tremendous application potential in 3D antennas. The relative permittivity of polymer-ceramic composites cannot increase to a very high value, even at maximum filler loading [53] since the 0–3 type composite follows an exponential relationship between relative permittivity of the composite and the volume fraction of the filler. At low volume fractions, the filler particles are randomly distributed in the polymer matrix with poor connectivity between the ceramic particles. At higher volume fractions or near the percolation threshold, the ceramic filler particles are connected, and hence the relative permittivity shows an abrupt increase. However, it is difficult to mix large amounts of ceramic fillers in the polymer matrix. It was found that the use of a coupling agent, such as silane treatment to modify the surface of the filler powders, although slightly improves the relative permittivity and mechanical properties, it degrades the microwave dielectric loss factor. The silane treatment is found to lower the porosity. The volume fraction of the ceramic that can be incorporated into the polymer depends on the density, powder particle size, and shape or morphology of the ceramic powder. When the powder particle size is very small, they have a high surface area, and only a small volume fraction can be incorporated.

## Rubber-Ceramic Composites for Flexible and Stretchable Applications

Recently electronic systems that can cover large areas on flexible substrates have received increasing attention because they enable wide range of applications such as flexible displays, electronic textiles, sensory skins, active antennas, etc. [54]. Devices based on this new technology are stretchable, twistable, and deformable into curvilinear shapes, thereby enabling applications that would be impossible to achieve by using the hard and rigid substrates [55]. Flexible electronics, an emerging field in electronic industry, enables a wide range of applications including capacitors for energy storage, antennas for wireless communication, electronic packaging, and electromagnetic interference (EMI) shielding. They can be folded and unfolded and fitted into non-planar forms for packaging or storage [46, 56]. The flexible substrates have many potential applications ranging from neural prosthetics in the medical field to microwave devices in electronics, which provides the advantage of three-dimensional designs of conformal structures [57, 58]. Conventional polymers filled with ceramic are rigid and cannot be bend or stretched. Stretchability means that the circuits should have the capacity to absorb large levels of strain without degradation in their electronic properties. In this context, the elastomer-ceramic composites can be used for stretchable and bendable electronic applications.

The requirements of a material to be used as a flexible dielectric are good mechanical flexibility, high thermal conductivity, low coefficient of thermal expansion, optimum permittivity (low $\varepsilon_r$ for fast signal speed and high $\varepsilon_r$ for miniaturization), good process ability, low dielectric loss, and low cost [46]. It is very difficult to identify a single material, which possess all these properties simultaneously. Butyl and silicone rubbers have low dielectric loss with good mechanical flexibility and stretchability, but they have low relative permittivity, low TC, and high CTE. By integrating the flexibility, stretchability, and low processing temperature of butyl and silicone rubbers with the high relative permittivity, low loss, and low CTE of ceramics [59], a composite may be formed, which can deliver improved performance. Composite electro ceramics introduce not only new functionalities but also an extremely wide range of properties that can be seamlessly adjusted in addition to a significant flexibility in fabrication. The relative permittivity of butyl rubber and silicone rubber can be tailored over a wide range by reinforcing with low-loss ceramics having different range of relative permittivity and volume fraction of the fillers in the rubber matrix [60].

In the pure form, silicone and butyl elastomers are thermoset polymer; once cross-linked they cannot be brought back to the former shape. Silicone and butyl rubber molecules exist above their glass transition temperature, and hence considerable segmental motions are possible. The glass transition temperature of silicone elastomer is about $-127\ ^\circ C$ and that of butyl rubber is about $-63\ ^\circ C$. The long polymer chains will cross-link during curing, and the process is known as vulcanization. Dicumyl peroxide is used for the vulcanization of silicone rubber and sulfur for butyl rubber. The elastomer exhibits large elongation from which they recover rapidly on the removal of the applied stress.

Recently Sebastian and co-workers reported [7, 59] the microwave dielectric properties of silicone and butyl rubbers filled with several ceramics of varying dielectric constants. The composites were prepared by hot pressing at 200 °C by applying a pressure of 2 MPa. The volume fraction of the ceramic that can be incorporated into the butyl rubber depends on the density, powder particle size, and shape or morphology of the ceramic powder. The addition of ceramic fillers in silicone and butyl rubbers gradually increased the relative permittivity. The increase in the relative permittivity depends on the amount of ceramic filler, its relative permittivity, and the frequency of measurement. As the relative permittivity of the fillers is higher than that of the elastomers, the $\varepsilon_r$ of the composites show an increasing trend with filler content. The microwave dielectric and physical properties of rubber-ceramic composites with the highest volume fraction with homogeneous dispersion of fillers are given in Tables 6 and 7. The loss tangent of the composite depends on the loss factor of the filler ceramics and is relatively small for alumna, silica, etc. since they are low-loss ceramics. The loss tangent increases considerably for $BaTiO_3$ since it is a lossy ferroelectric material. The composites are found to be flexible, bendable, and stretchable. The microwave dielectric and thermal properties are improved with ceramic loading. The composite preparation is difficult for ceramic loading higher than 40 vol.%. It is found that one can get only a relative permittivity of about 14 even with maximum loading with high-permittivity ceramics. The thermal conductivity increases, and coefficient of thermal expansion decreases with increase in filler content. The water absorption increases with increase in ceramic loading. The composites are found to have good dielectric properties and flexibility and are suitable for antenna fabrication and capacitive applications. One of the most attractive features of these particulate composites is that their electrical and physical properties can be varied over a wide range by choosing the appropriate volume fraction of the fillers in the rubber matrix.

**Table 6** Microwave dielectric, thermal, and physical properties of silicone rubber-ceramic composites (5 GHz) [7]

| Material | Average powder particle size μm | $V_f$ of filler | $\varepsilon_r$ | tan δ | CTE (ppm/°C) | TC (Wm$^{-1}$ K$^{-1}$) | Water absorption vol % |
|---|---|---|---|---|---|---|---|
| $SiO_2$ | 0.5 | 0.5 | 3.3 | 0.008 | 116 | 0.5 | 0.10 |
| $Al_2O_3$ | 2 0.0 | 0.4 | 5.7 | 0.009 | 114 | 1.6 | 0.34 |
| AlN | 1.3 | 0.4 | 4.7 | 0.017 | 138 | 1.0 | 0.10 |
| $Ba(Zn_{1/3}Ta_{2/3})O_3$ | 0.7 | 0.2 | 6.5 | 0.009 | 149 | 0.9 | 0.11 |
| $Ba(Mg_{1/3}Ta_{2/3})O_3$ | 0.5 | 0.2 | 5.1 | 0.011 | 152 | 0.4 | 0.11 |
| $BaTiO_3$ | 0.9 | 0.2 | 13.3 | 0.043 | 188 | 0.4 | 0.11 |
| $SrTiO_3$ | 0.8 | 0.3 | 14.2 | 0.011 | 142 | 1.0 | 0.08 |
| $Li_2ZnTi_3O_8$ | 0.7 | 0.3 | 7.4 | 0.009 | 144 | 0.8 | 0.11 |
| $Ca_{0.61}Nd_{0.26}TiO_3$ | 0.9 | 0.4 | 11.9 | 0.011 | 156 | 0.5 | 0.07 |

**Table 7** Microwave dielectric, thermal, and physical properties of butyl rubber-ceramic composites (5 GHz) [7, 59]

| Filler | Powder particle size | $V_f$ | $\varepsilon_r$ | tanδ | CTE | Water absorption (vol %) | TC W/mK |
|---|---|---|---|---|---|---|---|
| $SiO_2$ | <1 μm | 0.4 | 3.1 | 0.004 | 80 | 0.09 | 0.5 |
| $Al_2O_3$ | ~1 μm | 0.4 | 4.7 | 0.002 | 55 | 0.08 | 0.5 |
| $Ba(Zn_{1/3}Ta_{2/3})O_3$ | <1 μm | 0.3 | 5.8 | 0.002 | 86 | 0.05 | 0.3 |
| $Sr_2Ce_2Ti_5O_{16}$ | ~5 μm | 0.4 | 11.0 | 0.001 | 30 | 0.07 | 0.4 |
| $TiO_2$ | ~2 μm | 0.4 | 12.5 | 0.002 | 108 | 0.08 | 0.7 |
| $SrTiO_3$ | ~5 μm | 0.4 | 13.2 | 0.002 | 26 | 0.08 | 0.5 |
| $Ba_{0.7}Sr_{0.3}TiO_3$ | <5 μm | 0.3 | 13.1 | 0.009 | 29 | 0.06 | 0.4 |
| $BaTiO_3$ | ~1 μm | 0.3 | 12.7 | 0.020 | 33 | 0.12 | 0.4 |

## Radomes

A radome (radar dome) is a protective cover for the delicate antenna mounted on air vehicles, (airplanes, missiles, etc.) from severe surrounding environments such as the effects of humidity, high or low temperature, bird strike, insects, UV damage, wind, rain, or dust. Radomes are composed of panels that form a spherical shell to protect the enclosed antenna. The radomes equipped in supersonic or hypersonic aircraft may encounter high levels of mechanical and thermal loadings [61, 62]. For example, if the aircraft is flying at a velocity of more than 5 Mach, then radome has to withstand a high temperature of more than 1400 °C [63]. More importantly, the radome must not interfere with the utility of the antenna, which is responsible for communication, detection, or imaging [64]. A radome contains dielectric materials and sometimes paints layers. The important characteristics required for a radome material are:

(i)   The electromagnetic radiation should pass with the minimum transmission loss, and it depends on the materials dielectric constant and loss tangent.
(ii)  The material should be capable of being fabricated into a suitable structure, and this requires good knowledge of the material mechanical properties such as density, strength, and durability and should have the life lasting that of the vehicle in operation.
(iii) The material should withstand the thermal conditions, for which good knowledge of the material thermal conductivity, emissivity, thermal shock, and behavior with temperature change is improved.
(iv)  The material should withstand the environmental and contamination conditions without any degradation.

The high tensile strength and fracture toughness together with a low CTE prevent stress failures and suppress the formation and propagation of cracks resulting from erosive environment. A stable dielectric constant, with temperature, reduces bore

sight errors (BSE) caused by aerodynamic heating, and a low dielectric constant permits enhanced fabrication tolerance in wall thickness. The materials with good mechanical and thermal properties generally have higher dielectric constant. Hence, an optimal design for radome wall structures are needed for high temperature broad band applications. The radars are designed in the high frequency or microwave domain, and hence the thickness of the radome produces wavelength multiples which modifies the antenna patterns. Hence, the process of radar design should consider not only the radome structure but also the protective layers over it. A non-optimized radome can lead to several problems such as gain loss, bore sight errors (BSE), etc. degrading the radar range, ghost effects, artifact detections, or angular error detection. Thus, the importance of design and optimization of the radome layers for good transparency towards the antenna with minimum spurious reflections. Safety, security, and reliability are important features of communication, telemetry, and radar systems.

The EM wave undergoes two basic mechanisms of reflection and transmission when incident normally on a foreign medium which are governed by the following equations:

$$R = (Z_2 - Z_1)/(Z_2 + Z_1) \tag{1}$$

$$T = 2Z_2/(Z_2 + Z_1) \tag{2}$$

where

$R$ = reflection coefficient
$T$ = transmission coefficient
$Z_i$ = complex impedance of ith medium, which is given by:

$$Z = [j\,\omega\mu/(\sigma + j\,\omega\varepsilon_r)]_{1/2} \tag{3}$$

where

$Z$ = complex impedance of the medium
$\omega$ = angular velocity of the wave
$\mu$ = magnetic permeability of the material
$\sigma$ = electrical conductivity of the material

The materials required for the fabrication of radomes should be transparent to microwave in either a narrow- or a broadband of the EM spectrum. Equation (2) indicates the necessary condition for perfect transmission across a material (i.e., $T = 1$) and to ensure an impedance matching of the material with that of free space ($Z_2 = Z_1$). This actually eliminates any reflection loss from the surface. The dielectric constant $\varepsilon_r$ and the magnetic permeability $\mu$ (both real and imaginary part of each) of the material should be as low as possible to reduce the loss of microwave energy through the radome. In general, the radomes are made of non-magnetic materials, and so the importance is to reduce $\varepsilon'$ and $\varepsilon''$ of the materials and design them to be as close as possible to those of the free space ($\varepsilon_0 = 1 + j_0$). It may be noted that the radome performances are often also sensitive to the thickness of the

material. The radomes used in supersonic, in hypersonic, and for the reentry-type vehicles experience high skin temperatures. Hence, the materials should have, in addition to low dielectric constant and loss tangent, high glass transition temperature and good thermal and oxidation stability. Based on these requirements, the materials that qualify as candidates for different grades of airborne radomes can be broadly classified as ceramic based and polymer based.

The ideal radome material must be electrically very transparent to electromagnetic energy (a minimum power is lost on passing through the material) and should retain its physical integrity structurally throughout the entire flight trajectory under conditions of aerodynamic loads, thermal stresses, environmental conditions, and with long life with that of vehicle. The ideal radome material electrically is one which behaves as free space over all wavelengths. However, no such ideal material exists which will give the structural and physical protection to the vehicle. Hence finding a suitable material is difficult and is a compromise between electrical, thermal, and mechanical properties and physical requirements. There are a quite good number of low-loss materials satisfying radome requirements with varying dielectric constant, strength, working temperature range, etc. For example, a low dielectric constant may be considered for a wide frequency band application, whereas a high dielectric constant may be useful for a relative narrow frequency band with minimum aberration requirement. A high-density material such as alumina may be useful at high temperature. Lighter materials are available in resin-glass sandwich or solid laminate composites for the lower temperatures and ceramic-type materials for the higher temperatures.

## Ceramic-Based Radomes

The materials based on ceramics become critical for radome applications that have to withstand high temperatures ($\leq 400\ ^\circ$C) as in the cases of most supersonic/hypersonic missiles and spacecrafts. Each of these ceramic materials and their composites has their own advantages and disadvantages with respect to their dielectric properties, mechanical strength, thermal properties, and fabrication ease. The slip-cast fused silica (SCFS) stands out to be one of the best for high velocity applications (even up to Mach 8) for their favorable combinations of different properties like dielectric constant and loss, cost, CTE, etc. Most of the missile radomes are made of Pyroceram and slip-cast fused silica (SCFS). Other ceramics that have received attention or are being considered for advanced applications are Rayceram, nitroxyceram, reaction-bonded silicon nitride (RBSN), hot-pressed silicon nitride (HPSN), and celsian. Pyroceram 9606 and Rayceram8 are cordierites based and are composed of magnesia, silica, and alumina. Nitroxyceram contains silicon nitride, boron nitride, silica, and celsian barium oxide, alumina, and silica. RBSN and HPSN are made almost from silicon nitride along with small amounts of sintering additives. Slip-cast fused silica has excellent electrical performance and satisfactory mechanical performance but may erode considerably in a rain field. Nitroxyceram is promising, but it requires a difficult and expensive manufacturing process. The

**Table 8** List of important radome applications

|               | $\varepsilon_r$ | Loss tangent | Density gm/cm3 | Melting point | Hardness Mohs |
|---------------|------|-----------|-----------|---------|-------|
| Alumina       | 9.6  | 0.0001    | 3.7       | 2015    | 9     |
| Fused silica  | 3.7  | 0.0002    | 1.7       | 1680    | 6     |
| Pyroceram     | 5.6  | 0.0003    | 2.6       | 1350    | –     |
| Cordierite    | 6.2  | 0.0002    | 2.5       | 1435    | 7     |
| Boron nitride | 4.5  | 0.0004    | 2.0       | 2730    | 2     |
| Silicon nitride | 7.9 | 0.004    | 3.2       | 1900    | 7–9   |

**Table 9** Dielectric properties of polymers

| Material      | $\varepsilon_r$ | Loss tangent |
|---------------|---------|--------|
| Epoxy         | 3.4–4.0 | 0.02   |
| Polyester     | 2.8     | 0.003  |
| Polyimide     | 3.0     | 0.004  |
| Cyanate ester | 3.3     | 0.007  |
| Polycarbonate | 2.8–3.4 | 0.001  |
| PTFE          | 2.1     | 0.0001 |
| Polypropylene | 2.2     | 0.0003 |
| Polystyrene   | 2.5     | 0.0003 |

dielectric properties of some commonly used alumina, fused silica, cordierite, boron nitride, silicon nitride, Pyroceram ceramic-glass of Corning, etc. are given in Table 8. There are a large number of ceramics with excellent microwave dielectric properties (low dielectric constant and loss tangents). However, no investigation was reported for possible use as radomes. The reader is referred to the reference [7] for a list of low-loss dielectric materials.

## Polymer-Based Radome Materials

Some of the important polymers used for making radomes are given in Table 9. Quartz with $\varepsilon_r = 3.8$ and loss tangent 0.0002 and D-glass with $\varepsilon_r = 4.0$ and loss factor 0.0026 are usually used as reinforcement in the polymers. One can tailor the dielectric, thermal, and mechanical properties by selecting appropriate ceramic filler materials and their volume fractions in the polymer matrix.

Radomes for millimeter-wave applications were earlier made of pure thermoplastic polymer which nowadays are replaced with more advanced thermoplastics having superior resistances to rain erosion, moisture absorption, and impact loads. The thermoset resins are most commonly used for civilian and defense radomes, mainly owing to their easier processability, improved mechanical properties, and significantly lower coefficients of thermal expansion (CTE). It may be noted that some of the thermoset epoxy-based composites even withstand temperatures up to about 350 °C. Epoxy-based composites are extensively used for the aerospace industry. However, the relatively higher dipole activity and the presence of hydrogen

bonding result in a higher tan δ for epoxies. Moreover, the dielectric constant and loss tangent of these materials tend to increase further with increase in temperature. However, the epoxies or the polyesters are best to operate up to a temperature of 150 °C, which is often a major limitation for many applications. The thermoset polyimides, PTFE, and cyanate esters can withstand temperatures close to 300 °C. It must be noted that the final dielectric behaviors of the composites will depend on the amount and dielectric properties of the matrix resins and the reinforcements. Thus, both the polymer and the reinforced filler are important in determining the overall performance of the radomes. Polyurethane foams as dielectric materials are extensively used in the construction of radomes. Polyurethanes are commonly used as a composite material in land-based, space frame radomes. This is a cost-efficient solution enabling self-supporting radome panels that are hydrophobic and antimicrobial. Furthermore, two- and three-layer sandwich panels for desired thermal insulation can be formed. Polyurethanes are also used as composite materials in aircraft and as protective structures on leading edges of aircraft radomes to protect from erosion damage while ensuring proper signal from the aircraft antenna. Polyurethanes are especially useful in aerospace applications where functional, lightweight materials are imperative. There are several low $\varepsilon_r$ and low-loss polymer-ceramic and rubber ceramic composites reported in the literature and may be useful for radome applications [7].

## EMI Shielding Materials for Military and Aerospace Applications

Digital transformation is happening in aerospace and defense applications, platforms, and environments due to the increase of portable electronics devices and embedded electronic systems. They contribute a significant rise in RF emissions that could cause interference, data corruption, or mal functioning of devices. Aircraft, combat vehicles, ships, communication equipment, safety equipment, missile systems, and launchers – all platforms and vehicles, components, and systems need EMI/RFI shielding to operate functionally. Electronic warfare is a key component of battle space where electromagnetic emissions are used to interrupt or disrupt military equipment [65, 66]. For aerospace and defense applications, the requirements for EMI shielding will be more stringent as the shielding structure and material should also withstand potential high power EM attacks such as electromagnetic pulse (EMP) and electrostatic discharge (ESD), which can result in electrical short or dielectric breakdown [67, 68]. Germany developed a carbonyl iron powder loaded rubber sheet of thickness 0.3 inches and resonant frequency at 3 GHz named "Wesch" as a radar camouflage for submarines during World War II [69]. During this period, the USA developed materials known as "HARP" (Halpern Anti-Radiation Paint). MX-410, its airborne version, consists of base dielectric with high permittivity of 150 due to loading with highly oriented disk-shaped aluminum flakes suspended in a rubber matrix and carbon black. This material offered a 15–20 dB reduction in reflectivity in the X band [70, 71]. Shielding results of 20–35 dB may be sufficient to protect the interference resulted from low-power

consumer electronics but is not enough to meet EMI shielding requirements for defense and aerospace applications. Shielding of 50 dB and above is required for defense and aerospace applications [66, 72].

Effective EMI shielding is obtained with low surface resistance and high conductivity. There is an increase in the number and complexity of electronic equipment and the threat of electronic countermeasures (ECM), ranging from radar jamming and deception to a devastating electromagnetic pulse (EMP) attack. These aspects result in the need for greater protection from electromagnetic interference (EMI) and radio-frequency interference (RFI), which pose challenge to aerospace and defense engineers today and could have disastrous effects on safety and mission critical systems. Loss of a safety or mission critical system means somebody could die, a piece of equipment could be destroyed, or that the mission may failed. Hence, the demand for efficient shielding materials that are resilient to extreme environmental conditions, lightweight, and optically transparent while providing military-compliant shielding performance is on rise due to much more electromagnetic radiation in the air in comparison with a decade ago [65, 66].

## EMI Shielding Mechanism

Shielding of electromagnetic radiation is done by three mechanisms, viz., reflection, absorption, and multiple reflections. Reflection mechanism occurs in highly electrically conductive structures, such as metals, and relies on mobile charge carriers. Electric and/or magnetic dipoles in the shielding material can contribute to significant absorption of the waves. Attenuation by absorption depends on shield thickness, $\sigma_r$ and $\mu_r$. With increasing frequency, absorption increases, while reflection tends to decrease. Figure 5 shows the schematic representation of EMI shielding mechanism. Another mechanism is the multiple reflections that occur at surfaces or interfaces within the shield. This mechanism depends on the geometry of the materials, as it requires the presence of large surface areas or interfaces within the shield [72, 73].

## EMI Shielding Materials

Metallic shielding products have been in use for several years in the endless applications owing to the high attenuation it offers. Broadband absorbers have been made from solid metallic particles or dielectric-filled metallic dispersed in a matrix. Iron oxide, powdered iron, powdered aluminum and copper, silver, steel, evaporated metal or nickel chromium alloy, and metal wires are some of the conductive materials commonly used for high shielding applications [73, 74]. Table 10 gives a list of some of the reported metal-based EMI shielding materials. These materials are selected based on the measured high frequency and thickness less than 2 mm especially suitable for military and aerospace applications. Advanced composite materials are trying to replace metals in a wide range of applications mainly in aerospace due to its attractive properties like lightweight,

**Fig. 5** Schematic representation of EMI shielding mechanism
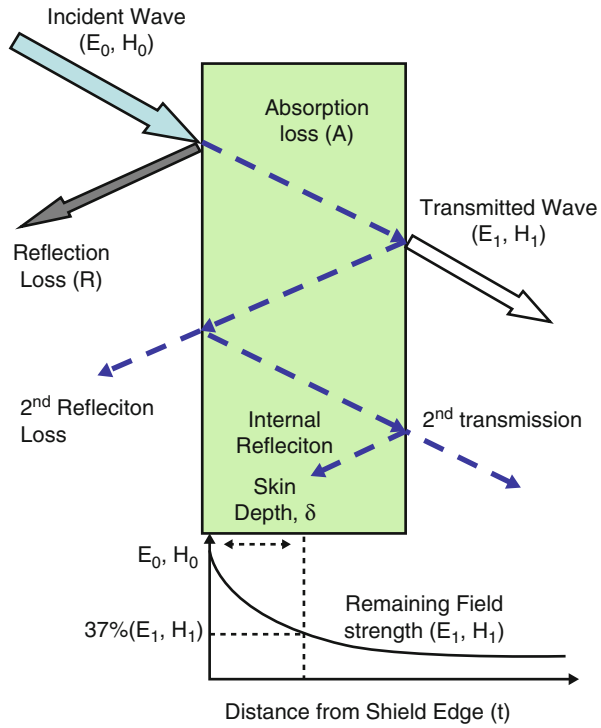


high stiffness, dimensional stability, and chemical/temperature resistance. One of the major obstacles is that these composite materials do not provide the shielding levels close to that of metals and is a major challenge in aircraft designs [73, 74, 104, 105]. Currently considerable interest is paid on the development of effective EMI shields based on carbon composites as an alternative to the metal-based shields in areas of aerospace, defense, automobiles, and next-generation flexible electronics owing to its unique properties of good electrical and thermal conductivity, as well as low density [72, 73]. Two-dimensional metal carbides and nitrides known as MXenes that combine metallic conductivity and hydrophilic surfaces are possible candidates owing to its good shielding properties with minimum thickness. Shahzad et al. reported $Ti_3C_2T_x$ film of 45 μm thick with EMI shielding effectiveness (EMI SE) of about 92 dB, which is highest among all synthetic materials of comparable thickness [106].

Recently, a promising EMI shielding material for the defense and aircraft industries is developed by Chaudhary et al. based on multiwall carbon nanotube (MWCNT)-mesocarbon microbead (MCMB) composite paper which has high conductivity and is lightweight and easily foldable by simple, efficient, and cost-effective strategy (Fig. 6). It is reported as the first efficient EMI shielding material in the X-band frequency region having low density of 0.26 g/cm$^3$ and absorption-dominated shielding effectiveness of 31 and 56 dB at 0.15–0.6 mm thickness,

**Table 10** Some of the reported materials having thickness less than 2 mm with good EMI SE in the high-frequency region

| SL No | Material | EMI SE dB | Frequency GHz | Ref |
|---|---|---|---|---|
| 1. | Cu deposited polymer substrate | 50–60 | 2–18 | [75] |
| 2. | Nanocrystalline Cu on Heat-treated polyaromatic hydrocarbons (HTPAHs) | 58.7 | 12.4–18 | [76] |
| 3. | Poly(vinyl chloride)/graphite/nickel Nanoconducting composites | 45–60 | 1–12 | [77] |
| 4. | Polyvinyl chloride reinforced graphite/copper nanoparticles | 22–70 | 1–20 | [78] |
| 5. | $Ti_3C_2T_x$ films | 90 | 8–12 | [79] |
| 6. | $Ti_3C_2T_x$-SA composites | 50–60 | 8–12 | [80] |
| 7. | MWCNT-mesocarbon microbead composite paper | 56 | 8–12 | [81] |
| 8. | Polyvinylidene fluoride-graphite flake composite | 55–57 | 8–18 | [82] |
| 9. | 10 wt% CNT/UHMWPE nanocomposite | 50 | 8–12 | [83] |
| 10. | Graphene foam/5 wt% CNT/PDMS composite | 70–80 | 8–12 | [84] |
| 11. | Graphene oxide-cellulose aerogel | 50–58 | 8–12 | [85] |
| 12. | ABS copolymer (Cycolac Ex39)/15 wt% MWCNT | 50 | 8.2 | [85] |
| 13. | Thermally reduced graphene oxide | 80.8 | 12.4–18 | [86] |
| 14. | PEEK/10 wt% expanded graphite | 57.9 | 10 | [87] |
| 15. | Polyaniline/5 wt% graphene | 51–52 | 2–12 | [88] |
| 16. | 5.7% multiwalled carbon nanotubes/ polydimethylsiloxane composites (MWNT/PDMS) | 70–80 | 8.2–12.4 | [89] |
| 17. | Poly(vinylidene fluoride) (PVDF) and multiwall carbon nanotubes (15 wt% MWCNTs) with three-dimensional (3D) networks | 50–70 | 8–12 | [90] |
| 18. | Polyimide/graphene composite foams | 51 | 8–12 | [91] |
| 19. | Exfoliated graphite | 130 | | [92, 93] |
| 20. | Acrylonitrile butadiene rubber/4 wt% graphene nanocomposites | 40–75 | 1–12 | [94] |
| 21. | Multilayer graphene anchored TiO2 in PPY matrix | 53 | 12.4–18 | [95] |
| 22. | 4.6 vol% multiwall carbon nanotubes (MWCNTs) within polypropylene random copolymer (PPCP) | 45–50 | 12.4–18 | [96] |
| 23. | Graphite-nanoferrite-fly ash composites | 40–98 | 8.2–12.4 | [97] |
| 24. | Graphene paper | 60 | 8–12 | [98] |
| 25. | Mesocarbon microsphere (MCMS) composite with $Fe_3O_4$ particles | 76 | | [99] |
| 26. | Carbon foam with SiC nanowires | 79 | 8.2 | [100] |
| 27. | Polypyrrole | 49 | 12–18 | [101] |
| 28. | Polyaniline nanofiber | 74 | 8.2–18 | [102] |
| 29. | Polyaniline nanofiber-2.3 wt.% of graphite flakes | 87 | 8.2–18 | [43] |
| 30. | 5 wt.% $Fe_3O_4$ in 10 wt.% PAN/DMF | 65–68 | 8.2–12.4 | [103] |
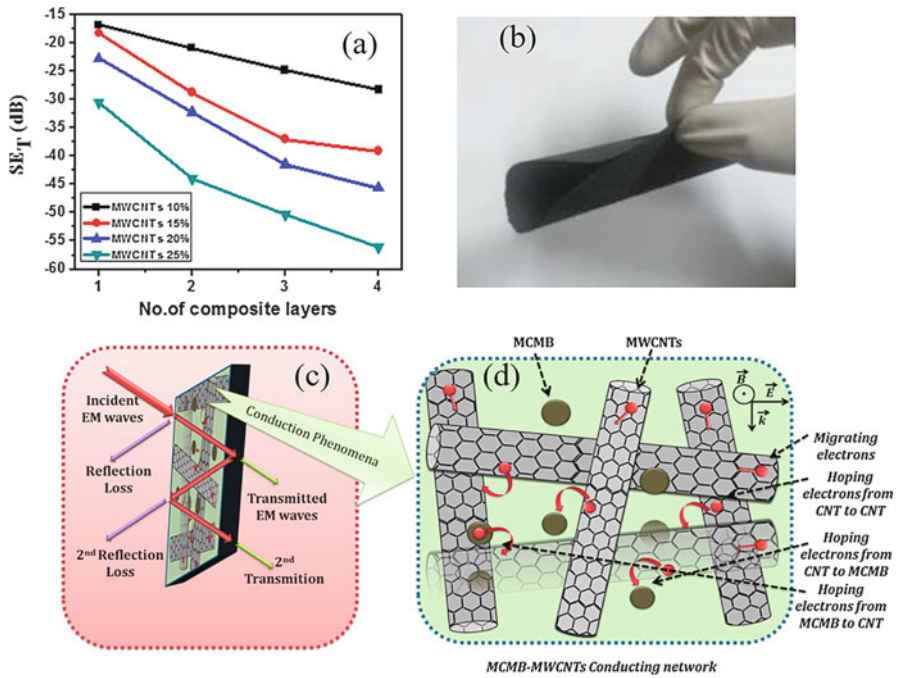
**Fig. 6**  (a) EMI shielding efficiency, (b) photograph, and (c, d) mechanism of MWCNT-MCMB composite paper. (Accessed from [81])
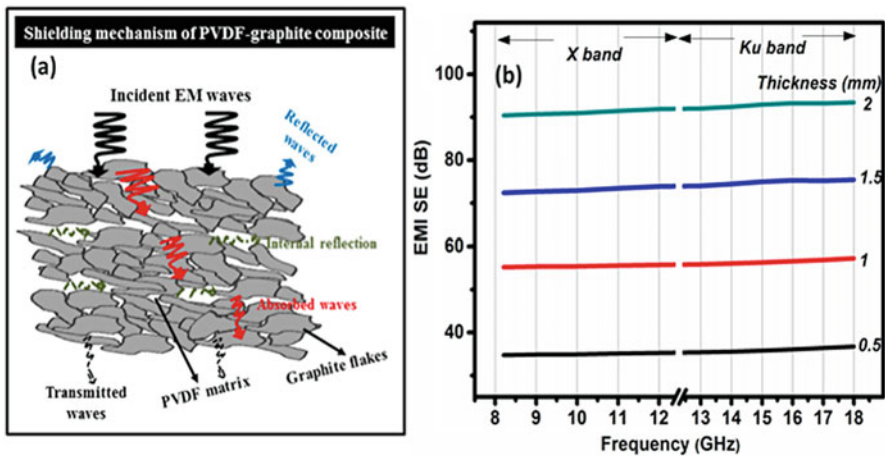


**Fig. 7**  Mechanism and EMI shielding efficiency of PVDF-70 vol% graphite composite. (Accessed from [82])
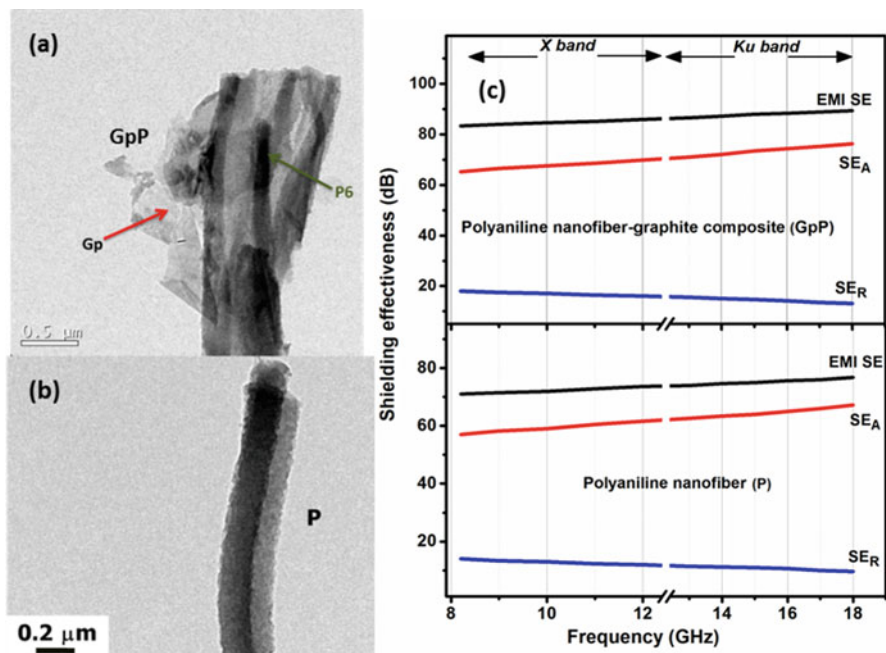
**Fig. 8** TEM images and EMI shielding efficiency of polyaniline nanofiber and its graphite composite. (Accessed from [102, 107])

respectively [81]. Joseph et al. reported polyvinylidene fluoride-graphite flake (Fig.7) composite of thickness 1 mm prepared by simple mixing and hot pressing method exhibits EMI SE of 55–57 dB in the 8.4–18 GHz frequency range [82]. Table 10 gives basic information on the research on the carbon-based high EMI shielding materials, which can be found useful for military and aerospace applications.

Another possible candidate to get good shielding materials is conducting polymers whose conductivity arises by the phonon-assisted hopping between randomly distributed localized states [43, 102]. The conducting polymers do not have great physical properties and are mostly used as composite of other materials such as latex, fibers, or polymer blends. The permittivity and permeability of conducting polymers can be controlled by synthetic means and hence are attractive electrical materials [43, 80, 102]. Figure 8 represents the microstructure and shielding properties of polyaniline nanofiber and its graphite composite. Electric-magnetic materials offer best potential candidates for thin broadband absorption but exhibit attenuation not enough for military and aerospace applications [108, 109]. The dielectrics are usually mixed with metal or carbon particles to get the desired shielding for these applications. Magnetic materials are limited to carbonyl iron and ferrites, which are prone to poor corrosion resistance [110]. It is more convenient to

use the EMI material as a paint, but not much attention was paid on this option [111]. Further research is needed in this area to make them useful for military and aerospace applications.

## Applications of Microwave Materials

Dielectric resonators using high-permittivity materials were initially developed for microwave circuits, such as filters and oscillators [112]. Later, Mcallister and Long [113] proposed the use of dielectric resonator as an antenna element. In recent years extensive work has been reported on dielectric resonator antenna (DRA) [114, 115]. Over the last two decades, two classes of antennas, i.e., the microstrip antenna and the DRA, have been extensively researched for modem wireless applications. Being low-loss (high Q) antennas, the microstrip antennas possess narrow bandwidth.

## Antennas

### Microstrip Antennas

Microstrip antennas, the most widely used types of antennas in the microwave frequency range, are often used in the millimeter-wave frequency range as well [116]. Below about 1 GHz, the size of a microstrip antenna is however usually too large for practical applications, and thus other types of antennas like wire antennas dominate. Also called patch antennas, microstrip patch antennas consist of a metallic patch of metal that is on top of a grounded dielectric substrate. The metallic patch may be of various shapes, with rectangular and circular being the most common. Microstrip antennas are suitable for space and missile applications due to their low profile, small size, lightweight, affordability, durability, and ease of fabrication and installation. They are structurally reliable due to their mechanical robustness withstanding also shock and vibration. In addition, they are conformable to a curved surface and feasible with the MMIC design, are versatile in terms of antenna parameters, and can be easily designed to produce linear or circular polarization with high gain. A typical substrate thickness is about 0.02 $\lambda_0$. Commercially available RT duroid, FR-4, Rogers, DuPont, Taconic, etc. substrates are commonly used for fabricating microstrip patch antennas. The DuPont 951 and 9 K7 LTCC are useful for applications in harsh adverse environments. The DuPont LTCC Green Tape™ 951 material system is designed for general applications up to 35 GHz. Green Tape™ 9 K7 is useful for high-frequency applications up to 100 GHz. A list of possible low-loss soft and hard dielectric materials with varying dielectric properties useful for microstrip antenna fabrication are given in Tables 1, 2, 3, 5, 6, and 7.

The dielectric constant has an impact on the dimension of microstrip conductors fabricated on the substrate material. Additionally, the dimensions are determined by the size of the fractional wavelengths (such as quarter wavelengths) of the signal frequencies to be carried by those circuit conductors. Thus, the dimensions decrease with the increasing frequencies. The dielectric constant also affects the dimensions

of microstrip conductors, shrinking their dimensions with increasing dielectric constant. Microstrip patch antenna is usually fabricated on substrates with a relative permittivity from 2.2 to 12. The higher the permittivity of dielectric material, the smaller the size of the antenna, but it achieves also lower efficiency and narrower bandwidth. This can play a role in the fabrication of a circuit and its conductor widths at higher frequencies. A lower dielectric constant is preferred at millimeter-wave frequencies, to avoid degradation of antenna properties. At higher frequencies, the use of thin samples results in finer conductor line widths for a controlled impedance line, such as the 50-Ohm lines commonly used in microwave circuits. Although thin dielectric materials may be attractive for making low-profile, lightweight PCBs, a thin microwave PCB with a high dielectric constant can result in extremely fine microstrip circuit dimensions. Also, the most compact microstrip antenna designs have decreased antenna gain due to the antenna size reduction. A high-permittivity substrate is used to fabricate compact microstrip patch antenna to overcome this disadvantage and obtain an enhanced antenna gain. If a substrate with a high permittivity is used for an antenna, achievable gain is 10 dBi with a smaller radiating patch. Conductor and dielectric losses become also more severe for thinner substrates. In addition, the surface wave losses become more acute for thicker substrate. Although the performance of microstrip antenna mainly depends on its structure and dimensions, the substrate material also has a significant role in performance such as reflection coefficient ($S_{11}$), bandwidth, etc. Thus, the microstrip antenna is usually narrowband, with typical bandwidths of a few percent. The patch antennas also tend to have lower radiation efficiency than some other types, with efficiencies typically between 70% and 90%. Anyway, they are widely used in mobile communications, satellite communications, direct broadcast service, remote sensing, biomedical radiators, and military systems such as missile, rockets, aircraft, etc. In addition, for spacecrafts and missiles applications, the ceramic antennas are more preferred than the ones based on polymer composites since environment is often harsh with large temperature variations. A large number of papers on antenna design and applications using different materials of varying dielectric constants are available in open literature, and the reader is referred to these books for details [117–120].

Ultra-wide band (UWB) technology has extremely wide operating bandwidth but has very low emission level which limits the wireless connection range to a few meters. Hence, the UWB radiotechnology is more likely to be applied in consumer electronics such as handset/laptop-centric and home networks which require short range but high data-rate wireless solutions. UWB systems will coexist with other traditional communication systems in the same frequency band by using low power levels. Recently considerable amount of interest has been paid on the possibility of developing antennas that employ fractal geometry in their design. Fractals can be used to miniaturize patch elements as well as wire elements. Recently, new forms of fractal antennas (combination of fractal geometry) are proposed for miniaturization, WLAN, and UWB applications.

**Dielectric Resonator Antenna**

To confine radiation and maintain a high-quality factor important for filter and oscillator applications, the ceramic dielectric resonators are often enclosed inside metal cavities. However by removing the metallic shield and suitable feeding to excite appropriate mode, the resonators could become efficient radiators being thus feasible for antenna applications as proposed by McAllister and Long [112]. The reader is referred to the recent reviews related to these dielectric resonator antennas (DRA) [115, 121, 122]. The DRA is constructed from dielectric resonator, substrate, and ground with different excited feeding techniques. DRA consists of dielectric materials as its radiating patch also called as DR on one side of the substrate and has a ground plane (metal) on the other side. DRA is a resonant antenna, fabricated from low-loss microwave dielectric material. There is no inherent conductor or surface wave loss in dielectric resonators which leads to high radiation efficiency. In case of DRA, various modes are excited to produce a broadside or omnidirectional radiation pattern for different coverage requirements. Simple coupling schemes can be used for DRA to most of the transmission lines used in microwave and millimeter-wave frequencies. Experimental and theoretical studies are extensively done on DRA with different shapes or geometries. The dimensions of the DRA ($D$) are related to the free space resonant wavelength ($\lambda_0$) by the approximate relation $D \, \alpha \, \lambda o \varepsilon_r^{-0.5}$ and by choosing a high $\varepsilon_r$; the size of the DRA can be significantly reduced at the expense of bandwidth. The operating bandwidth can be varied for a wide frequency range by suitably selecting the resonator parameters, and a bandwidth of 140% has been reported [123]. The lowest frequency of DRA reported is 55 MHz [124] and the highest 94 GHz [125]. DRAs with dimensions ranging from a few millimeters with $\varepsilon_r$ in the range of 6–100 have been reported [115, 121, 122]. The use of a wide range of dielectric permittivity values allows the designer to have control over size and bandwidth, i.e., wide bandwidth is achievable using low permittivity, and compact size is achievable with high permittivity. Very thin (<4 mm) structures are needed especially when integrated to portable terminals. Ceramic dielectric materials are widely used for GPS patch antennas leading to high performance and miniaturization. Ceramic antennas have also been proposed for multipurpose targets like machine-to-machine communication [126]. The DRAs are characterized by low phase noise, compact size, frequency stability with temperature, ease of integration with other hybrid MIC circuitries, simple construction, and the ability to withstand harsh environments. It has some interesting characteristics like lightweight, high permittivity, wide impedance bandwidth, low production cost, and ease of excitation.

The impedance bandwidth is a function of the dielectric constant and dimensions of the sample. Higher dielectric constant facilitates size reduction, whereas lower dielectric constant increases the bandwidth. In the millimeter-wave frequency range, the DRA are smaller size than the conventional antennas by a factor of square root of the dielectric constant of the material ($\varepsilon_r$). The DRA has also high radiation efficiency (>95%) because of the absence of losses due to conductor or surface wave, increased bandwidth, low cost, and compatibility to planar antenna feeding

techniques. The DRA has wider impedance bandwidth as compared to microstrip antenna. A bandwidth of 10% can be achieved for a dielectric constant of ten or less for a rectangular DRA. It must be also noted that the microstrip antenna radiates through two narrow edges of the patch, while the DRA radiates through its entire surface except the grounded portion. Surface waves are also absent in the DRA in contrast to the microstrip antenna thus improving the efficiency and reducing distortions in the radiation pattern. The DRA can have different shapes such as conical, tetrahedral, hexagonal, pyramidal, elliptical, and stair-stepped shapes or hybrid antenna designs using dielectric resonator antennas in combination with microstrip patches, monopoles, or slots. Extensive work has been reported on designing dielectric resonator antennas for applications like WiMAX, WLAN applications, UWB applications, RFID, and all dielectric wireless receivers. The size of antenna can be reduced by increasing the relative permittivity of the material making it viable for low-frequency operations. However excessive miniaturization may degrade the efficiency and BW of antenna. The radiation efficiency of a dielectric resonator antenna is not significantly affected by its dielectric constant, and a wide range of values can be used. However, the bandwidth of the DRA is inversely related to the dielectric constant and may limit the choice of values for a given application. An antenna with high gain must be larger in size with low Q-factor and therefore will have a higher BW. As the size of the antenna decreases, the effective aperture size is reduced, lowering directivity. A high-permittivity DRA can be used as a small and low-profile antenna. The DRAs made from high dielectric constant materials have a single resonant frequency with a well-defined internal field structure and hence do not have the bandwidth required for modern communication systems. Several designs such as mono DRA, poly DRAs, hybrid DRAs, annular ring DRA, parasitic DRA, etc. have been reported to achieve bandwidth enhancements for DRAs [125]. Recently, Antenova Ltd., UK, has developed a pair of lightweight, flexible antennas with better than 75% efficiency which can provide radio links to navigation satellites, as well as in wireless connectivity bands such as Bluetooth and Wi-Fi, for IoT and M2M applications. The properties of several DRA geometries with different permittivity and feeding are given in Tables 11 and 12.

**Metamaterial-Based Antennas**
The recent growth in telecommunication increased the demand for small and versatile antennas for multifunctional systems such as cell phones, handheld portable wireless devices for Internet connection, short- and long-range communication devices, radio-frequency identification (RFID), etc. Similarly small equipment and devices used for data transmission and navigation (GPS systems) require small antennas with omnidirectional radiation patterns. For reducing antenna size and volume, traditional miniaturization methods such as shorting pins, meandering, and dielectric loading [132] are adopted. This often results in low radiation efficiency, narrow bandwidth, and undesired radiation patterns. Therefore, in recent years, a strong interest has been generated on using periodic structures (metamaterials) to lower antenna profile as a method to optimize or enhance antenna performance. Metamaterials are typically constructed from periodic arrangements of

**Table 11**  Mono DRA designs [122, 127–131]

| S. N | DRA geometry | Relative permittivity ($\varepsilon_r$) | Feed mechanism | ~BW % |
|---|---|---|---|---|
| 1 | Flipped staired pyramid | 12 | Slot | 62 |
| 2 | Strip-fed rectangular | 9.8 | Conducting strip | 43 |
| 3 | Inverted L shaped | 9.2 | Probe | 38 |
| 4 | Cylindrical DRA | 12 | Probe | 30 |
| 5 | Half hemispherical | 10 | Probe | 35 |
| 6 | Cylindrical cup | 10.2 | L-shaped probe | 32 |
| 7 | Two-step stair shaped | 12 | Slot square cross section | 54 |
| 8 | Rectangular with an offset well | 20 | Slot | 18 |
| 9 | U shaped | 9.8 | Elliptical patch | 72 |
| 10 | Rectangular with a tunnel | 20 | Slot | 20 |
| 11 | H shaped | 9.8 | Trapezoidal patch | 62 |
| 12 | L shaped | 9.8 | Conformal inverted trapezoidal patch | 71 |
| 13 | Rectangular high aspect ratio (5.2:1) | 25 | Microstrip line | 16 |
| 14 | Rectangular with a moat | 20 | Slot | 35 |
| 15 | Cylindrical | 10 | Conformal metallic strip connected to SMA probe | 66 |
| 16 | Rectangular placed on a concave ground plane | 9.8 | Probe | 55 |
| 17 | Embedded multi-segment rectangular | 9.8 | Vertical feeding strip | 50 |
| 18 | Trapezoidal | 10 | Probe | 55 |
| 19 | Cylindrical | 10.2 | Dual coaxial probe | 68 |
| 20 | Bowtie | 9.8 | Probe | 49 |
| 21 | Cylindrical | 10.5 | Narrow slot in a rectangular waveguide | 20 |
| 22 | Circular disk | 10.5 | Waveguide probe | 50 |
| 23 | Rectangular on a conductor backed CPW | 48 | Coplanar | 8 |
| 24 | Rectangular | 48 | L strip | 17 |
| 25 | Elliptical | 48 | T strip | 14 |
| 26 | Seven element log periodic | 2.1,6,9.8,10,10.2 | Microstrip line | 92 |
| 27 | Capacitive coupled log periodic | 2.1 | Microstrip series feed | 65.2 |
| 28 | Nine element log periodic | 12 | Microstrip line | 95 |

conventional materials to exhibit electromagnetic properties not found in any of their bulk individual constituents. An early boost to this research was the initial experimental verifications of electromagnetic bandgap structures (EBGs) and negative refractive index media (NRI or equivalently $\epsilon<0$ and $\mu<0$ media). Printed circuit realizations of metamaterials led to smaller radio-frequency (RF) devices such as

**Table 12** Monopole UWB DRA geometries and properties [123, 132–141]

| S. N. | Geometry | $\varepsilon_r$ | Operating frequency GHz | BW |
|---|---|---|---|---|
| 1 | Annular ring DRA centrally excited by λ/4 monopole | 10 | 6.0–18.0 | 3:1 |
| 2 | Eye-shaped monopole DRA excited by coaxial probe connected to SMA connector | 10 | 3.0–20.0 | 6:1 |
| 3 | Annular DRR excited by T-shaped monopole | 10 | 4.5–16.0 | 3.5:1 (112%) |
| 4 | Pawn-shaped DRR excited by λ/4 monopole | 10 | 5.5–22.0 | 4:1 |
| 5 | Inverted truncated annular conical DRA excited by monopole | 9.8 | 3.4–5.0 | – |
| 6 | Conical DRR excited by λ/4 monopole | 10 | 5.7–23 | 4:1 |
| 7 | Hemispherical DRR excited by λ/4 monopole | 10 | 5.7–23 | 4:1 |
| 8 | Stepped radius annular DRR excited by λ/4 monopole | 10 | 3.0–10.3 | 110% |
| 9 | Mushroom-shaped DRR with three materials | 4, 5, 7 | 4–25 | 137% |
| 10 | Mushroom-shaped DRR | 2.1 | 3–4 | 137% |
| 11 | Annular DRR loaded monopole | 10 | 5–20 | 100% |
| 12 | Inverted conical DRR-loaded monopole + skirt-shaped ground plane | 10 | 4–15 | 111% |
| 13 | Annular DRR loaded t-shaped monopole | 10 | Probe | 112% |
| 14 | Pawn-shaped DRR loaded monopole | 10 | Probe | 122% |
| 15 | Conical and hemispherical DRA-loaded monopole | 10 | Probe | 126% |
| 16 | Stacked conical DRR | 10 | Probe | 138% |
| 17 | Stacked annular DRR | 2.2 | Probe | 140% |

phase shifters, couplers, and antennas. Introduction of metamaterials into the antenna system can provide exciting challenges for antenna engineers to meet the need for an increasing demand for military and space systems [141].

### Low-Temperature Co-fired Ceramics Antennas

The recent advances in aerospace technologies demand new ways to package electronics for high temperature and harsh environments, the low-temperature co-fired ceramic (LTCC). LTCC is a multilayer design and packaging system that can embed passive components and thermal management structures within a substrate. LTCC packaging techniques uses stacked layers of a ceramic dielectric material to create printed circuit boards with embedded passives (such as thick-film resistors and capacitors), embedded heat sinks, and hermetic sealing using Kovar-TM lids. The low loss and relatively high dielectric constant of the LTCC materials make them desirable for high-frequency applications and are discussed in section "HTCC and LTCC Substrate/Packages." Low-temperature co-fired ceramics (LTCC) have become an attractive technology for miniaturization of portable electronic devices and have been used for packaging integrated circuits (ICs) and applied

to actuators, sensors, and integrated microsystems with relatively low cost and high productivity. The LTCC-based multilayer technology has an extensive range of applications in areas such as telecommunications, automotive, aeronautics, radio-frequency (RF) modules (mobile phone, Bluetooth (2.4 GHz), Home RF, IEEE 802.11), microwave modules, optoelectronic modules, global positioning systems (GPS, 1.6 GHz), broadband access connection systems (5.8−40 GHz), and medical, military, and sensors packaging [142].

Antennas have been designed at different frequencies using the LTCC technology [143] approach ranging from 1 to 270 GHz. LTCC antenna in IEEE 802.15.3c band shows a vast area of applications. For example, LTCC Ferro A6M materials are used for ($\varepsilon_r$ = 5.9, tan$\delta$ = 0.002) the above band. In some designs the microstrip line antenna is using a silver conductor on the top surface of the LTCC substrate having a ground plane for antenna on the bottom surface. The permittivity of the substrate used is $\varepsilon_r$ = 7.8 and tan$\delta$ = 0.002. For multiple-frequency GSM band of 900/1800 MHz (lowest known frequency), LTCC technology is also implemented. Here LTCC tapes with dielectric constant and loss tangent value ($\varepsilon_r$ = 7.8, tan$\delta$ = 0.0047), respectively, are used to integrate the monopole helix antenna. LTCC technology is also used in electronically steerable antennas. Steerable antennas are the antennas that can change or steer its beam to the desired direction at a particular angle. This beamforming technique can be used for transmission and reception.

LTTC-based antenna is also designed with broadband and high gain at 60 GHz band, which is the internationally allocated band for communication. This antenna is designed with a substrate RNE5M ($\varepsilon_r$ = 6, tan$\delta$ = 0.0035). Nowadays LTCC-based ultra-wideband antenna [144] is also gaining interest among researchers. In this regard, LTCC substrate (type GL-550) with a dielectric constant of 5.7 (tan$\delta$ = 0.0006) is considered for designing UWB antenna to reduce the size of frontend modules in wireless transceivers. The future broadband wireless communication systems will have the need for more bandwidth in order to satisfy the increasing demands to achieve higher data rates. In this sense, the millimeter-wave frequency band will play a key role in fifth-generation (5G) wireless cellular networks. Here LTCC-based dielectric flat lens antennas and switched-beam arrays are very much effective for future 5G millimeter-wave communication systems. In order to design the LTCC lens prototypes dielectric material, DuPont 9 k7 ($\varepsilon_r$ = 7.1, tan$\delta$ = 0.0009) is used. With this design there can be scanning of high-gain radiation in both azimuth and ($\varepsilon_r$ = 7.1, tan$\delta$ = 0.0009) elevation planes, necessary for supporting high data transmission (>1.5 Gbps) as it is recommended in the IEEE 802.15.3c standard [142, 145]. It also helps in avoiding the requirement of high number of RF switches to perform such 2D radiation pattern configuration.

LTCC-based antennas can be designed to best suit modern-day miniaturized communication devices operating almost anywhere in the frequency spectrum, and the performance of the antenna can be improved by using different permittivity materials. Hence, it is a better choice for future wireless communication applications and an even more viable option compared with other traditionally used integration technologies. The DuPont 9 k7 material has been shown to perform well up to 100 GHz. The LTCC in general has a lower thermal expansion coefficient and higher

flexural strength, varying relative permittivity and low loss tangent and good thermal conductivity than polymer-based composites. LTCC-based circuits have an extensive range of applications in areas such as telecommunications, automotive, aeronautics, radio-frequency (RF) modules (mobile phone, Bluetooth, Home RF, IEEE 802.11), microwave modules, optoelectronic modules, and medical, military, and sensors packaging.

## Dielectric Resonator Filters

High-performance DR filters are widely used in wireless and satellite communication systems due to their superior characteristics, such as high unloaded Q, excellent temperature stability, and smaller size compared to their air-filled counterpart [146–149]. Temperature-stable high-Q dielectric materials with a wide range of dielectric constants from 4 to 100 are available [6, 7]. Two types of dielectric-loaded resonator filters are commonly used:

(a) Dual-mode filter, operating in $HE_{11}$ mode, providing low loss, smaller volume, and elliptic function realizations. Here only half the number of physical cavities is needed.
(b) Single-mode filter with all resonators operating in $TE_{01\delta}$ mode, providing low loss, flexible layout structure, and better spurious-free performance.

The drawback of the dielectric-loaded resonator filters is their inferior spurious characteristics, especially in the dual-mode configuration. By mixing the $TE_{01\delta}$ and $HE_{11}$ modes in filter realization with proper cavity design, the spurious performance of the DR filter can be improved while maintaining the advantages of elliptic function filters. The dual-mode filter can halve the number of physical resonator cavities, therefore significantly reducing the weight and volume of the unit. It has been widely used in satellite communication systems. $TE_{01}$single-mode filters offer the advantages of design simplicity and flexibility in layout options over $HE_{11}$ dual-mode filters, while dual-mode filters have significant advantages in the mass and volume of the products. Mixing the $TE_{01}$ and $HE_{11}$ modes, dielectric-loaded resonator filters achieve the advantages of dual mode $HE_{11}$ DR filters and the excellent spurious performances of the $TE_{01}$ mode ring resonator filters [148].

In recent works the designing of balanced/balun filters with differentially feeding method to DR is accomplished [147]. Similarly, triple-mode dielectric resonator is machined from a single piece of Trans-Tech 3500 series ceramic dielectric material with a dielectric constant of 35. This triple-band dielectric filter offers high Q and is miniature in size in comparison to previously reported multiband filter designs. This also allows independent control of each coupling matrix parameters [146]. The design of a high-efficiency filter-integrated class-F power amplifier (PA) in which high-Q-factor dielectric resonator (DR) filter is employed as the output matching network of the class-F PA shows excellent performance. It employs the dielectric material with $\varepsilon_r = 38$, $\tan\delta = 0.0002$, respectively, for designing the filter [149].

## Dielectric Resonator Oscillators

Oscillators producing energy at microwave frequencies are an essential component in most microwave communication systems, such as communication links, radar, frequency synthesizers, and so on. The dielectric resonator when coupled with two or three terminal active devices provides a vehicle for producing high-quality fixed frequency or narrowband tunable oscillators. A dielectric resonator (DR) can be used to form the stabilizing element in an oscillator. The dielectric resonator oscillators (DRO) are known as one of the most suitable devices for generating low-cost microwave signals. Dielectric resonator oscillators (DROs) are characterized by the following properties: high-frequency stability, high efficiency, and low manufacturing cost [150]. They also can be made to provide good temperature stability. The key elements to be optimized with respect to oscillator performance are output power, start-up stability, phase noise, DC-RF efficiency, tuning range, sensitivity to DR placement, and frequency pushing/pulling. In order for microwave oscillation to begin, a means to overcome the resistive losses in the circuit has to be provided. These losses include undesired stray and parasitic resistances and also the load into which the oscillator must operate (usually 50 $\Omega$). To do this the concept of negative resistance is introduced. If the amount of negative resistance exactly cancels the sum of the positive resistances, then the circuit will have a resonant or oscillation frequency where the inductive reactance is equal to the capacitive reactance. This condition is known as the steady-state oscillation condition. In order for oscillation to build up, an excess of negative resistance is required. Then, any small perturbation in the circuit, such as electrical noise, will kick-start a resonance. As oscillation builds the amount of negative resistance decreases until the steady-state condition is met. A negative resistor can be formed from an unstable active device with suitable feedback applied. Dielectric resonators can be used in both negative resistance (reflection) and feedback-type oscillators. The property of being easily coupled to a microstrip line is another reason to use dielectric resonators on integrated circuits.

The DRO design provides many types of active devices. For example, GaAs technology is considered as one of the most suitable transistor for microwave applications because of its frequency stability against temperature variation and its low noise characteristic. On the other hand, GaAs MESFET [151] is able to offer better performance than GaAs FET. As the dielectric resonator, Trans-Tech 8300 series dielectric resonator ($\varepsilon_r = 35.5$) is used. The unloaded quality factor of this resonator can be up to 15,000. The design of Ka-band monolithic differential launcher for mode excitation integrated with the cylindrical DR ($\varepsilon_r = 30.51$) monolithic differential DRO using SiGe technology shows excellent performance [152].

## Conclusion

Microwave dielectric materials play a key role in global society, with a wide range of applications straddling terrestrial and satellite communications although the first real devices were reported only 50 years ago. The recent progress in the IoT, microwave

telecommunications, satellite broadcasting, and intelligent transport systems (ITSs) has resulted in an increasing demand for low-loss dielectric materials and EMI shielding materials. Low-loss dielectric materials are extensively used in wireless communication systems as well as in several electronic devices. There are a large number of materials reported in the literature, and ideal materials should be judiciously selected depending on the applications. The fast progress in microwave materials is mainly due to the demands critical for defense and aerospace applications being in the forefront of the research. These demands include, e.g., low permittivity with high Qf values for resonators and antennas, much higher EMI shielding performance, and good stability of the dielectric properties in harsh and hostile environments not so severe in the common wireless communication. The emerging microwave materials in the forms of inks, composites, and foams are expected to form solutions also in the future. Conformable, bendable, or stretchable shielding, resonating, or radiating devices are on the way, but further research is needed especially for defense and aerospace applications where the high-frequency performance is less negotiable than in the other areas.

# References

1. Richtmeyer R (1939) Dielectric resonators. J Appl Phys 15:391–398
2. Okaya A (1960) The rutile microwave resonator. T Proc IRE 48:1921–1921
3. Cohen S (1968) Microwave band pass filters containing high Q dielectric resonators. IEEE Trans Microw Theory Tech MTT-16:1628–1629
4. Masse DJ, Purcel RA, Ready DW, Maguire EA, Hartwig C (1971) A new low loss high K temperature compensated dielectric for microwave applications. Proc IEEE 59:1628–1629
5. Wakino K, Nishikawa T, Tamura S, Ishikawa Y (1975) Microwave bandpass filters containing dielectric resonators with improved temperature stability and spurious response. IEEE-MTT-S Int Microw Symp Dig, Palo Alton, CA, 63–65
6. Sebastian MT (2008) Dielectric materials for wireless communication. Elsevier, Amsterdam
7. Sebastian MT, Ubic R, Jantunen H (2017) Microwave materials and applications. Two Volume sets John Wiley & Sons Inc., West Sussex
8. Sebastian MT, Ubic R, Jantunen H (2015) Low-loss dielectric ceramic materials and their properties. Int Mater Rev 60(7):392–412
9. Jain T (2013) Technology advancement in wireless communications. Int J Sci Technol Res 2 (8):2277–8616
10. Seraphim DP, Feinberg I (1981) Electronic packaging evolution in IBM. IBM J Res Dev Res Dev 25:617–618
11. Tummula PK (1996) Microelectronic packaging handbook. Springer, New York
12. Varghese J (2016) Zircon based hard. LAP LAMBERT Academic Publisher, Soft Microwave Substrates and Devices
13. Ralf R, Patrick S, Martin O (2014) SMTR® module – evolution towards Airborne Applications. International Radar Conference-2014, https://doi.org/10.1109/RADAR.2014.7060400
14. Schuh H (2009) X-band T/R-module front-end based on GaN MMICs. Intern J Microw Wirel Technol 1:387–394
15. Yu H, Liu J, Zhang W, Zhang S (2015) Ultra-low sintering temperature ceramics for LTCC applications: a review. J Mater Sci Mater Electron [Internet]:1–10. Springer. Available from: http://link.springer.com/10.1007/s10854-015-3282-y
16. Jin Y, Wang Z, Chen J (2010) Introduction to microsystem packaging technology. CRC Press, Boca Raton

17. Chen L-Y, HiTEC, HiTEN, & CICMT (2014), Vol. 2014, No. HITEC, pp. Dielectr. Perform. a High Purity HTCC Alumina High Temp. – a comparison study with other polycrystalline alumina," Additional Conferences Device Packaging HiTEC, HiTEN, & CICMT; January 2014, p 000271–7

18. Chen L-Y, Neudeck PG, Hunter G (2016) Electrical Performance of a High Temperature 32-I/O HTCC Alumina Package. 21000 Brookpark Road Cleveland, Ohio 44135 2 NASA Glenn Research Center, 21000 Brookpark Road, Cleveland, Ohio 44135

19. Blackwell E, Raton B (2000) The electronic packaging handbook. Press CRC, Boca Raton

20. Harper C (2000) Electronic packaging and interconnection handbook, 3rd edn. McGraw-Hill, New York

21. Varghese J, Vahera T, Ohsato H, Iwata M, Jantunen H (2017) Novel low-temperature sintering ceramic substrate based on indialite/cordierite glass ceramics. Jap J Appl Phys 56:10PE01

22. Varghese J, Joseph T, Sebastian MT (2011) $ZrSiO_4$ ceramics for microwave integrated circuit applications. Mater Lett 65(7):1092–1094

23. Pullanchiyodan A, Surendran KP (2016) Formulation of Sol–Gel derived bismuth silicate dielectric ink for flexible electronics applications. Ind Eng Chem Res:7108–7115. Available from: http://pubs.acs.org/doi/abs/10.1021/acs.iecr.6b00871

24. Arun S, Sebastian MT, Surendran KP (2017) $Li_2ZnTi_3O_8$ based high κ LTCC tapes for improved thermal management in hybrid circuit applications. Ceram Int 43(7):5509–5516

25. Ferro Corporation (2015) Low temperature co – fired ceramic systems A6M/A6M – E high frequency LTCC tape system [Internet]. Tech. data sheet LTCC. 2015. pp 1–2. Available from: http://www.ferro.com/Our+Products/ColorsGlass/Electronic/Electronic-Materials/docs/A6M-E LTCC Tape System.pdf

26. Dupont. LTCC [Internet]. Datasheet (2017) (cited 1 Jan 2017). Available from: http://www.dupont.com/content/dam/dupont/products-and-services/electronic-and-electrical-materials/documents/prodlib/GreenTape_Design_Layout_Guidelines.pdf

27. Thomas D, Abhilash P, Sebastian MT (2013) Casting and characterization of $LiMgPO_4$ glass free LTCC tape for microwave applications. J Eur Ceram Soc 33(1):87–93

28. Roshni SB, Sebastian MT, Surendran KP (2017) Can zinc aluminate-titania composite be an alternative for alumina as microelectronic substrate? Sci Rep[Internet] 7:40839. Nature Publishing Group; Available from: http://www.nature.com/articles/srep40839

29. Kaneko T, Watanabe H, Akaishi M, Wada K (1999) AlN HTCC super miniaturized millimeter wave transceiver MCMs, the novel structure for the high reliability, the high performance and the mass productivity. IEEE MlT-S Dig 2:449–452. (0–7803–5135–5/99/$10.00 0 1999 IEEE)

30. Cressler JD, Mantooth HA (2013) Extreme environment electronics. Chapters 1–5. CRC Press, Boca Raton\Florida, pp 1–47

31. Spry DJ, Neudeck PG, Chen L, Lukco D, Chang CW, Beheim GM, Krasowski MJ, Prokop N (2016) Processing and characterization of thousand-hour 500 °C durable 4H-SiC JFET integrated circuits. In: Proceedings of the 2016 IMAPs international conference on high temperature electronics (HiTEC 2016). International Albuquerque, New Mexico

32. Catalog Smt (2017) HTCC QFN Packages to 40 GHz [Internet]. 2017 [cited 1 Jan 2017]. p 1. Available from: https://smtnet.com/company/index.cfm?fuseaction=view_company&company_id=47300&component=catalog&catalog_id=19408

33. Dupont (2009) DuPont™ Green Tape™ 951 Technical Datasheet. 2009;3

34. Sebastian MT, Jantunen H (2008) Low loss dielectric materials for LTCC applications: a review. Int Mater Rev 53:57–90

35. Sebastian MT, Wang H, Jantunen H (2016) Low temperature co-fired ceramics with ultra-low sintering temperature: a review. Curr Opin Solid State Mater Sci 20:151–170

36. Suresh EK, Prasad K, Arun NS, Ratheesh R (2016) Synthesis and microwave dielectric properties of $A_{16}V_{18}O_{61}$ (a = Ba, Sr and ca) ceramics for LTCC applications. J Electron Mater 45(6):2996–3002

37. Varghese J, Ramachandran P, Sobocinski M, Vahera T, Jantunen H (2019) ULTCC glass composites based on rutile and anatase with co-firing at 400 °C for high frequency applications. ACS Sustain Chem Eng 7(4):4274–4283

38. Joseph N, Varghese J, Teirikangas M, Sebastian MT, Jantunen H (2018) Ultra-low sintering temperature ceramic composites of CuMoO 4 through Ag 2 O addition for microwave applications. Compos Part B 141:214–220

39. Joseph N, Varghese J, Teirikangas M, Sebastian MT, Jantunen H (2016) Glass-free CuMoO4 ceramic with excellent dielectric and thermal properties for ultralow temperature co-fired ceramic applications. ACS Sustain Chem Eng 4(10):5632–5639

40. Varghese J, Surendran KP, Sebastian MT (2014) Room temperature curable silica ink. RSC Adv 4(88):47701–47707

41. Varghese J, Teirikangas M, Puustinen J, Jantunen H, Sebastian MT (2015) Room temperature curable zirconium silicate dielectric ink for electronic applications. J Mater Chem C 3(35): 9240–9246

42. Joseph AM, Nagendra B, Bhoje Gowd E, Surendran KP (2016a) Screen-printable electronic ink of ultrathin boron nitride Nanosheets. ACS Omega 1(6):1220–1228

43. Joseph N, Sebastian MT (2016) A facile formulation and excellent electromagnetic absorption of room temperature curable polyaniline nanofiber based inks. J Mater Chem C 4:999–1008

44. Liu W, Wang H, Zhou D, Li K (2010) Dielectric properties of low-firing $Bi_2Mo_2O_9$ thick films screen printed on Al foils and alumina substrates. J Am Ceram Soc 93(8):2202–2206

45. Pullanchiyodan A, Surendran KP (2016) Formulation of sol–gel derived bismuth silicate dielectric ink for flexible electronics applications. J Eur Ceram Soc 36(8):1939–1944

46. Sebastian MT, Jantunen H (2010a) Polymer-ceramic composites of 0-3 connectivity for circuits in electronics: a review. Int J Appl Ceram Technol 7(4):415–434

47. Wall L (1972) Fluoropolymers. Wiley, New York

48. Willis OR (2008) Characterizing fluroropolymeric materials for microelectronics and MEMS packaging, ProQuest Information and Learning Company, USA

49. Bur A (1985) Dielectric properties of polymers at microwave frequencies: a review. Polymer (Guildf) 26:963–977

50. Allen F, Robert L, Michael E (1996) Ceramic filled composite polymeric electrical substrate materials exhibiting high dielectric constant and low thermal coefficient of dielectric constant

51. Allen FHIII (1994) Fluoropolymeric electrical substrate material exhibiting low thermal coefficient of dielectric constant, US Patent No. 5358775

52. Sebastian MT, Krupka J, Arun S, Kim CH, Kim HT (2018) Polypropylene-high resistivity silicon composite for high frequency applications. Mater Lett (232):92–94

53. Popielarz R, Chiang C (2007) Polymer composites with dielectric constant comparable to that of barium titanate ceramics. Mater Sci Eng B 139:48–54

54. Sun Y, Rogers J (2007) Inorganic semiconductors for flexible electronics. Adv Mater 19:1897–1916

55. Rogers J, Huang Y (2009) A curvy, stretchy future for electronics. Proc Natl Acad Sci 106:10875–10876

56. Seol Y, Noh H, Lee S (2008) Mechanically flexible low-leakage multilayer gate dielectrics for flexible organic thin film transistor. Appl Phys Lett 93:013305–1–013305–3

57. Gubbels F, Jaeger R, Gleria M (2007) Silicones in industrial applications. In: Jaeger R, Gleria M (eds) Inorganic polymers. Nova Science Publishers, New York, pp 61–162

58. Yang S, Jiang K (2012) Elastomer Application in Microsystem and Microfluidics. In: Boczkowska A (ed) Advanced elastomers – technology, properties and applications. InTech. Open Science mind, Rijeka, pp 203–222

59. Sebastian MT, Chameswary J (2016) Flexible and stretchable electronic composites, springer series on polymer and composite materials. In: Ponnamma D (ed) Poly(Isobutylene-co-Isoprene) compos flex electron appl. Springer International Publishing, Switzerland, pp 335–365

60. Sebastian MT, Ananthalumar S, Subodh G, Juuti J, Teirinkangas M, Jantunen H (2012) Composite electroceramics. In: Nicolais L, Borzacchiello A (eds) Wiley encyclopedia of composites, 2nd edn. Wiley, Inc., Boston

61. Amin A, Sierakowski R (1990) Effect of thermomechanical coupling on the response of elastic solids. AIAA J 28(7):1319–1322
62. Dasgupta S (2015) Polymer matrix composites for electromagnetic applications in aircraft structures. J Indian Inst Sci 952:75–296
63. Chen F, Shen Q, Zhang L (2010) Electromagnetic optimal design and preparation of broadband ceramic radome material with graded porous structure. Prog Electromagn Res 105:445–461
64. Hong T, Song M-Z, Liu Y (2011) RF directional modulation technique using a switched antenna array for communication and direction-finding applications. Prog Electromagn Res 120:195–213
65. Military aerospace (2011) Shielding-against-electromagnetic-and-rf-interference-for-safety-and-mission-success [Internet]. Technol. Focus. 2017 [cited 20 Jul 2011]. Available from: http://www.militaryaerospace.com/articles/print/volume-28/issue-7/technology-focus/shielding-against-electromagnetic-and-rf-interference-for-safety-and-mission-success.html
66. Chauhan S, Abraham M, Choudhary V (2016) Superior EMI shielding performance of thermally stable carbon nanofiber/poly(ether-ketone) composites in 26.5–40 GHz frequency range. J Mater Sci 51:9705–9715
67. Pascucci N. (2016) EMI shielding caulk delivers superior performance in military radar systems, [internet]. Available from: www.parker.com/chomerics
68. Wen B, Cao M, Lu M, Cao W, Long H, Wang X et al (2014) Reduced graphene oxides light weight and high efficiency electromagnetic interference shielding at elevated temperatures. Adv Mater 26:3484–3489
69. Saville P (2005) Review of Radar Absorbing Materials. RDC Atl. TM 2005-003
70. Halpern O (1960) Method and means for minimizing reflection of high frequency radio waves, US Patent No. 2923934
71. Halpern O, Johnson MHJ, Wright RW (1960) Isotropic absorbing layers, US Patent No. 2951247
72. Joseph N, Singh S, Sirugudu R, Murthy V, Ananthakumar S, Sebastian MT (2013) Effect of silver incorporation into PVDF-barium titanate composites for EMI shielding applications. Mater Res Bull 48:1681–1687
73. Chauhan S, Abrahamand M, Choudhary V (2016) Electromagnetic shielding and mechanical properties of thermally stable poly (ether ketone) multiwalled carbon nanotube composites prepared using twin screw extruder equipped with novel fractional mixing elements. RSC Adv 6(2016):113781–113790
74. Klemperer C, Maharaj D (2009) Composite electromagnetic interference shielding materials for aerospace applications. Compos Struct 91:467–472
75. Byeon J, Kim J-W (2011) Aerosol based fabrication of a Cu/polymer and its application for electromagnetic interference shielding. Thin Solid Films 520:1048–1052
76. Kumar A, Singh A, Kumari S, Dutta P, Dhawan S, Dhar A (2014) Polyaromatic-hydrocarbon-based carbon copper composites for the suppression of electromagnetic pollution. J Mater Chem A 2:16632
77. Al-Ghamdi AA, El-Tantawy F, Aal N, El-Mossalamy E, Mahmoud W (2009) Stability of new electrostatic discharge protection and electromagnetic wave shielding effectiveness from poly(vinyl chloride)/graphite/nickel nanoconducting composites. Polym Degrad Stab 94:980–986
78. Al-Ghamdi A, El-Tantawy F (2010) New electromagnetic wave shielding effectiveness at microwave frequency of polyvinyl chloride reinforced graphite/copper nanoparticles. Compos Part A 41:1693–1701
79. Shahzad F, Alhabeb M, Hatter C, Anasori B, Hong SM, Koo C et al (2016) Electromagnetic interference shielding with 2D transition metal carbides (MXenes). Science 353:1137–1140
80. Skotheim TA, Elsenbaumer R, Reynolds JR (1998) Handbook of conducting polymers. Marcel Dekker, New York

81. Chaudhary A, Kumari S, Kumar R, Teotia S, Singh B, Singh A et al (2016) Lightweight and easily foldable MCMB-MWCNTs composite paper with exceptional electromagnetic interference shielding. ACS Appl Mater Interfaces 8:10600–10608

82. Joseph N, Varghese J, Sebastian MT (2017a) Graphite reinforced polyvinylidene fluoride composites an efficient and sustainable solution for electromagnetic pollution. Compos Part B Eng 123:271–278

83. Al-Saleh M (2015) Influence of conductive network structure on the EMI shielding and electrical percolation of carbon nanotube/polymer nanocomposites. Synth Met 205:78–84

84. Sun X, Liu X, Shen X, Wu Y, Wang Z, Kim J-K (2016) Graphene foam/carbon nanotube/poly (dimethyl siloxane) composites for exceptional microwave shielding. Compos Part A 85:199–206

85. Al-Saleh M, Saadeh W, Sundararaj U (2013) EMI shielding effectiveness of carbon based nanostructured polymeric materials: a comparative study. Carbon NY 60:146–156

86. Kumar R, Dhawan S, Singh H, Kaur A (2016) Charge transport mechanism of thermally reduced graphene oxide and their fabrication for high performance shield against electromagnetic pollution. Mater Chem Phys 180:413–421

87. Goyal R (2013) Cost-efficient high performance polyetheretherketone/expanded graphite nanocomposites with high conductivity for EMI shielding application. Mater Chem Phys 142:195–198

88. Modak P, Kondawar S, Nandanwar D (2015) Synthesis and characterization of conducting polyaniline/graphene nanocomposites for electromagnetic interference shielding. Procedia Mater Sci 10:588–594

89. Theilmann P, Yun D-J, Asbeck P, Park S-H (2013) Superior electromagnetic interference shielding and dielectric properties of carbon nanotube composites through the use of high aspect ratio CNTs and three-roll milling. Org Electron 14:1531–1537

90. Wang H, Zheng K, Zhang X, Ding X, Zhang Z, Bao C et al (2016) 3D network porous polymeric composites with outstanding electromagnetic interference shielding. Compos Sci Technol 125:22–29

91. Li Y, Shen B, Pei X, Zhang Y, Yi D, Zhai W et al (2016) Ultrathin carbon foams for effective electromagnetic interference shielding. Carbon NY 100:375–385

92. Luo X, Chugh R, Biller BC, Hoi Y, Chung D (2002) Electronic applications of flexible graphite. J Electron Mater 31(5):535–544

93. Luo X, Chung D (1996) Electromagnetic interference shielding reaching 130 dB using flexible graphite. Carbon NY 34:1293–1299

94. Al-Ghamdi A, Al-Ghamdi A, Al-Turki Y, Yakuphanoglu F, El-Tantawy F (2016) Electromagnetic shielding properties of graphene/acrylonitrile butadiene rubber nanocomposites for portable and flexible electronic devices. Compos Part B 88:212–219

95. Gupta A, Varshney S, Goyal A, Sambyal P, Gupta B, Dhawan S (2015) Enhanced electromagnetic shielding behavior of multilayer graphene anchored luminescent $TiO_2$ in PPY matrix. Mater Lett 158:167–169

96. Verma P, Saini P, Malik R, Choudhary V (2015) Excellent electromagnetic interference shielding and mechanical properties of high loading carbon nanotubes/polymer composites designed using melt recirculation equipped twin-screw extruder. Carbon NY 89:308–317

97. Mishra M, Singh A, Dhawan S (2013) Expanded graphite–nanoferrite–fly ash composites for shielding of electromagnetic pollution. J Alloys Compd 557:244–251

98. Zhang L, Alvarez N, Zhang M, Haase M, Malik R, Mast D et al (2015) Preparation and characterization of graphene paper for electromagnetic interference shielding. Carbon N Y 82:353–359

99. Dhawan R, Kumari S, Kumar R, Dhawan S, Dhakate S (2015) Mesocarbon microsphere composites with $Fe_3O_4$ nanoparticles for outstanding electromagnetic interference shielding effectiveness. RSC Adv 5:43279

100. Farhan S, Wang R, Li K (2016) Electromagnetic interference shielding effectiveness of carbon foam containing in situ grown silicon carbide nanowires. Ceram Int 42:11330–11340

101. Kaur A (2012) Ishpal, Dhawan S. tuning of EMI shielding properties of polypyrrole nano-particles with surfactant concentration. Synth Met 162:1471–1477
102. Joseph N, Varghese J, Sebastian MT (2015) Self-assembled polyaniline nanofibers withenhanced electromagnetic shielding properties. RSC Adv 5:20459–20466
103. Bayat M, Yang H, Ko F, Michelson D, Mei A (2014) Electromagnetic interference shielding effectiveness of hybrid multifunctional $Fe_3O_4$/carbon nanofiber composite. Polymer (Guildf). 55:936–943
104. Cabrera C, Miranda F (2015) Advanced nanomaterials for aerospace applications. CRC press, Taylor and Francis group
105. Joseph N, Janardhanan C, Sebastian MT (2014) Electromagnetic interference shielding properties of butyl rubber-single walled carbon nanotube composites. Compos Sci Technol 1:139–144
106. Tong X (2009) Advanced materials and design for electromagnetic interference shielding. CRC Press, Taylor and Francis group, Now York
107. Joseph N, Varghese J, Sebastian MT (2016) A facile formulation and excellent electromagnetic absorption of room temperature curable polyaniline nanofiber based inks. J Mater Chem C 4:999–1008
108. Joseph N, Varghese J, Sebastian MT (2017b) In situ polymerized polyaniline nanofiber-based functional cotton and nylon fabrics as millimeter-wave absorbers. Nat Polym 49:391–399
109. Zhou P, Chen J, Liu M, Jiang P, Li B, Hou X-M (2017) Microwave absorption properties of $SiC@SiO_2@Fe_3O_4$ hybrids in the 2–18 GHz range. Int J Miner Metall Mater 24:804–813
110. Kong L, Li Z, Liu L, Huang R, Abshinova M, Yang Z et al (2013) Recent progress in some composite materials and structures for specific, electromagnetic applications. Int Mater Rev 58:203
111. Folgueras L, Alves M, Rezende M (2010) Microwave absorbing paints and sheets based on carbonyl iron and polyaniline: measurement and simulation of their properties. J Aerosp Technol Manag 1:63–70
112. Kajfez D, Guillon P (1986) Dielectric resonators. Artech House, Norwood
113. Mcallister M, Long S (1983) Rectangular dielectric resonator antenna. IEEE Electron Lett 19:218–219
114. Luk K, Leung K (2002) Dielectric resonator antennas. Electronic & electrical engineering research studies series. Research Studies Press, Taunton
115. Petosa A (2007) Dielectric resonator antenna handbook. Artech House, Boston
116. Garg R, Bhartia P, Bahl I, Ittipiboon A (2000) Microstrip antenna design hand book. Artech house Inc., Norwood
117. Garg R (2001) Microstrip antenna design handbook. Artech house Inc., Norwood
118. Imbriale W (ed) (2006) Spaceborne antennas for planetary exploration. Wiley, Hoboken
119. Kumar G, Ray K (2003) Broadband microstrip antennas. Artech House, Boston
120. Pozar D, Schaube D (eds) (1995) Microstrip antennas: the analysis and design of microstrip antennas and arrays. Institute of Electrical and Electronics Engineers, New York
121. Petoso A, Ittipiboon A (2010) Dielectric resonator antennas. A historical review and the current state of the art. IEEE Antennas Propag Mag 52:91–116
122. Soren D, Ghatak R, Mishra R, Poddar D (2014) Dielectric resonator antennas: designs and advances. Progr Electromag Res B 60:195–213
123. Ozzaim C (2014) Monopole antenna loaded by stacked annular ring dielectric resonators for ultrawide bandwidth. Microw Opt Technol Lett 56:2395–2398
124. Kingley S, OKeefe S (1999) Beam steering and monopulse processing of probe fed dielectric resonator antenna. Proc Rada Sonar Navig 3:121–125
125. Svedin J, Huss L, Karlen D, Enoksson P, Rusu C (2007) A micromachined 94 GHz dielectric resonator antenna for focal plane array applications. In: IEEE international microwave symposium, Honolulu, –IEEE MTT-S, pp 1375–1378
126. Liflander J (2010) Ceramic chip antennas vs. PCB trace antennas: a comparison. MPDIGEST [Internet]. 2010; Available from: Feature article, White paper, www.pulseelectronics.com/download/3721/g041/pdf

127. Bijumon P, Menon S, Lethakumari B, Sebastian MT, Mohanan P (2006) Broad band elliptical dielectric resonator antennas excited with geometry modified microstrip lines. Microw Opt Technol Lett 48:65–67

128. Kumari R, Behera S (2014) Investigation on log periodic dielectric resonator antenna array for Ku band applications electromagnetics. Electromagnetics 34(1):19–33. Taylor Francis

129. Kumari R, Behera S (2013b) Nine element frequency independent dielectric resonator array for X- band applications. Microw Opt Technol Lett 55(2):400–403

130. Menon S, Lethakumary B, Bijumon P, Sebastian M, Mohanan P (2005) L-strip fed wide band rectangular dielectric resonator antenna. Microw Opt Technol Lett 45:227–228

131. Suma M, Menon S, Bijumon P, Sebastian M, Mohanan P (2005) Rectangular dielectric resonator antenna on a conductor -backed co-planar waveguide. Microw Opt Technol Lett 45(2):154–156

132. Caloz C, Itoh T (2006) Electromagnetic metamaterials: transmission line theory and microwave applications. Piscataway, Wiley

133. Ganguly D, Guha D, George S, Kumar C, Sebastian M, Antar Y (2017) New design approach for hybrid monopole antenna to achieve increased ultra-wide bandwidth. IEEE Antennas Propag Mag 11:139–144

134. Ghosh S, Chakrabarty A (2008) Ultrawide band performance of dielectric loaded T-shaped monopole transmit and receive antenna/EMI sensor. IEEE Antennas Wirel Propag Lett 7:358–361

135. Guha D, Gupta B, Antar Y (2012) Hybrid monopole-DRAs using hemispherical/conical-shaped dielectric ring resonators: improved ultrawide band designs. IEEE Trans Antennas Propag 60:393–398

136. Guha D, Gupta B, Antar Y (2009) New pawn-shaped dielectric ring resonator loaded hybrid monopole antenna for improved ultrawide bandwidth. IEEE Antennas Wirel Propag Lett 8:1178–1181

137. Guha D, Antar Y, Ittipiboon A, Petosa A, Lee D (2006) Improved design guidelines for the ultra wideband monopole-dielectric resonator antenna. EEE Antennas Wirel Propag Lett 5:373–377

138. Jazi M, Denidni T (2008) A new hybrid skirt monopole dielectric resonator antenna. In: Proceedings of the IEEE antennas propagation society international symposium, pp 1–4

139. Kumari R, Behera S (2013c) Mushroom shaped dielectric resonator antenna for WiMAX applications. Microw Opt Technol Lett 55:1360–1365

140. Ozzaim C, Ustuner S, Tarim N (2013) Stacked conical ring dielectric resonator antenna excited by a monopole for improved ultrawide bandwidth. IEEE Trans Antennas Propag 61:1435–1438

141. Sheeja K, Behera S, Sahu P (2012) Bandwidth improvement of a zeroth order resonant antenna for WiMax applications. Int J RF Microw Comput Eng 22(4):569–574

142. Ullah U, Ain M, Mahyuddin N, Othman M, Ahmad Z, Abdullah M et al (2015) Antenna in LTCC technologies: a review and the current state of the art. IEEE Antennas Propag Mag 57:241–260

143. Kim D, Kang D, Shin M, Jung H, Lim J (2016) Design of a low temperature co-fired ceramic (LTCC) based antenna with broadband and high gain at 60 GHz bands. In: IEEE international conference on consumer electronics Asia. ICCE-Asia, pp 1–3

144. Abbosh A, Bialkowski M, Jacob M, Mazierska J (2005) Investigations into an LTCC based ultra-wide band antenna. In: Asia-Pacific microwave conference (APMC), p 4

145. Imbert M (2017) Assessment of LTCC based dielectric flat lens antennas and switched beam arrays for future 5G millimeter – wave communication systems. IEEE Trans Antennas Propag 65:6453–6473

146. Li J, Zhan Y, Qin W, Wu Y, Chen J-X (2017) Differential dielectric resonator filters. IEEE Trans Compon Packag Manuf Technol 7:637–645

147. Qin W, Chen J-X (2017) Balanced/balun filters based on dielectric resonators. In: IEEE global symposium on millimeter-waves

148. Wang ZK (2007) Dielectric resonators and filters. IEEE Microw Mag 8:115–127

149. Zhu L, Mansour R, Yu M (2017) Triple-band dielectric resonator bandpass filters. In: IEEE MTT-S international microwave symposium. pp 745–747
150. Webster J (1999) Dielectric resonator oscillators. In: Wiley encyclopedia of electrical and electronics engineering. Wiley, Chichester
151. Ugurlu S (2011) Dielectric resonator oscillator design and realization at 4.25 GHz. In: International conference 2011, p II-205-II-208
152. Hamed K, Freundorfer A, Antar Y (2007) A monolithic differential coupling mechanism for dielectric resonators excitation in conductive silicon substrates. IEEE Microw Wirel Components Lett 17:25–27